

## REVIEW OPEN ACCESS

# Current Trends and Future Prospects of Integrating Electrospinning With 3D Printing Techniques for Mimicking Bone Extracellular Matrix Scaffolds

Kardo Khalid Abdullah<sup>1</sup>  | Kolos Molnár<sup>1,2,3</sup> 

<sup>1</sup>Department of Polymer Engineering, Faculty of Mechanical Engineering, Budapest University of Technology and Economics, Budapest, Hungary | <sup>2</sup>HUN-REN-BME Research Group for Composite Science and Technology, Budapest, Hungary | <sup>3</sup>MTA-BME Lendület Sustainable Polymers Research Group, Budapest, Hungary

**Correspondence:** Kolos Molnár ([molnar@pt.bme.hu](mailto:molnar@pt.bme.hu))

**Received:** 4 November 2024 | **Revised:** 6 January 2025 | **Accepted:** 20 January 2025

**Funding:** This work was supported by the National Research, Development, and Innovation Office, FK 138501 and Nemzeti Kutatási, Fejlesztési és Innovációs Alap, TKP2021-EGA.

**Keywords:** 3D printing | biopolymer | ECM | electrospinning | nanofiber | tissue engineering

## ABSTRACT

This article presents a review of the recent findings on the combination of electrospun nanofibers and three-dimensional (3D)-printed structures for extracellular matrix (ECM) scaffolds for bone tissue engineering. We explore the synergy between electrospinning (ES), which produces highly porous, fibrous structures from materials like collagen and gelatin, and 3D printing, which allow precise scaffold design using biopolymers. We discuss the selection of appropriate biopolymers based on their mechanical properties, biocompatibility, and biodegradability, as well as the key functions of ECM structures in cell attachment, migration, and differentiation. We analyze the strengths and limitations of each technique, noting that while ES enhances cellular adhesion and proliferation, it struggles with complex geometries and scalability. In contrast, 3D printing provides strong structural support but faces challenges with resolution and biomaterial compatibility. Our review focuses on the innovative integration of these methods, aiming to merge ES's microstructural precision with 3D printing's structural strength. We evaluate various hybrid combination methods, including sequential and coaxial techniques, and discuss potential solutions to challenges related to ECM scaffold quality, production time, and scalability. Furthermore, we highlight recent discoveries and propose future research directions to enhance further mimicking the ECM scaffold of bone.

## 1 | Introduction

In the context of bones, the extracellular matrix (ECM) refers to the complex network that comprises the structural framework of bone tissues [1]. It primarily consists of fibrous, non-soluble, and high-molecular-weight proteins like collagen and proteoglycans [2], as shown in Figure 1. Together, they serve as a scaffold and offer mechanical support to bone cells [4, 5], which support is significant for ensuring the strength and integrity of bone [6].

Additionally, ECM provides adequate space and surface for cell attachment, migration, and differentiation.

The ECM can undergo damage from various factors such as mechanical impact, aging, illness, or inflammation [7]. Tissue regeneration is a medical approach that blends materials science, biology, and engineering to guide the recovery of damaged tissues and organs [8, 9] and encourages seamless integration with the host tissue [10]. Hence, the primary objective in tissue

This is an open access article under the terms of the [Creative Commons Attribution-NonCommercial](https://creativecommons.org/licenses/by-nc/4.0/) License, which permits use, distribution and reproduction in any medium, provided the original work is properly cited and is not used for commercial purposes.

© 2025 The Author(s). *Journal of Polymer Science* published by Wiley Periodicals LLC.

engineering (TE) is to make a suitable ECM scaffold capable of offering basic structural support, as we outlined. Recently, various methods have been used to repair damaged bone ECM scaffolds to promote bone regeneration. These include treatments like bone grafting, growth factor therapy, stem cell therapy, and TE [11, 12].

In the field of TE, primary techniques such as three-dimensional (3D) printing and electrospinning (ES) are commonly used in research to reproduce ECM structures. The ES technique is a feasible method for generating polymeric nanofiber mats. Besides, 3D printing has emerged as a powerful technique for creating customized shapes with precise control over geometry and pore structures. In addition, various polymers and biopolymers, including natural and synthetic polymers, are being widely used in those techniques.

Despite that, each technique has unique challenges in replicating ECM structures. The ES method, in particular, is limited

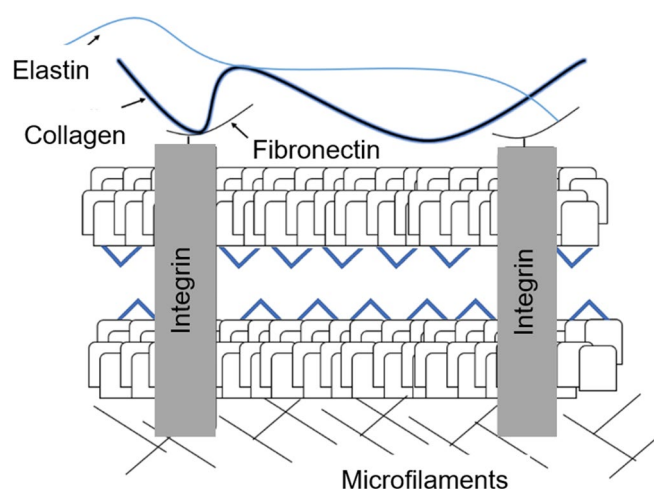


**FIGURE 1** | The structure and components of the ECM. This figure is based on the work by M. Keshvardoostchokami et al., titled Electrospun nanofibers of natural and synthetic polymers as artificial ECM for tissue engineering and is licensed under the Creative Commons Attribution 4.0 International License (CC BY 4.0). The original work can be found in reference [3].

by the flat structure of its products [13]. Some simple multilayered structures can be achieved by stacking electrospun fibers with varying compositions [14]. However, electrospun layers cannot truly replicate the spatial structure of ECMs, rendering them insufficient to address substantial bone defects' restorative needs [15].

Consequently, the main features of electrospun nanofibers are high surface area [16], substantial porosity [17], and exceptional absorption capabilities [18]. Additionally, nano- or microscale fibers, mainly from biopolymers, can be produced through ES techniques to simulate the fibrous nature inside ECM.

Similarly, in the 3D printing technique, achieving adequate resolution and precision in such a complex bone ECM structure stands as a challenge. The 3D printing technology has diverse methods offering unique capabilities for precise and reproducible geometry on the macro level. Henceforth, this combination provides enhanced surface customization, creation of gradient structures, expedited prototyping, and precise control over pore size and porosity. In the following chapters, our objective is to summarize and review existing literature findings on how the ES technique, biopolymers employed, and various methods of 3D printing serve as valuable means for mimicking ECM structures.

Integrating the advantages of both techniques holds great potential in TE for creating personalized 3D scaffolds. The combination of ES and 3D printing technologies presents a connection between the unique properties of electrospun nanofibers and the unique design freedom of 3D printing. In the following chapters, we review each technique and the related ECM-mimicking approaches in detail.

## 2 | ES Methodology

The positive benefits of electrospun nanofiber structures have encouraged researchers to explore their applications further in various fields related to TE [19], wound healing [20], drug delivery [21], and other branches such as filtration [22], sound absorption [23], and chemical sensors [24, 25].

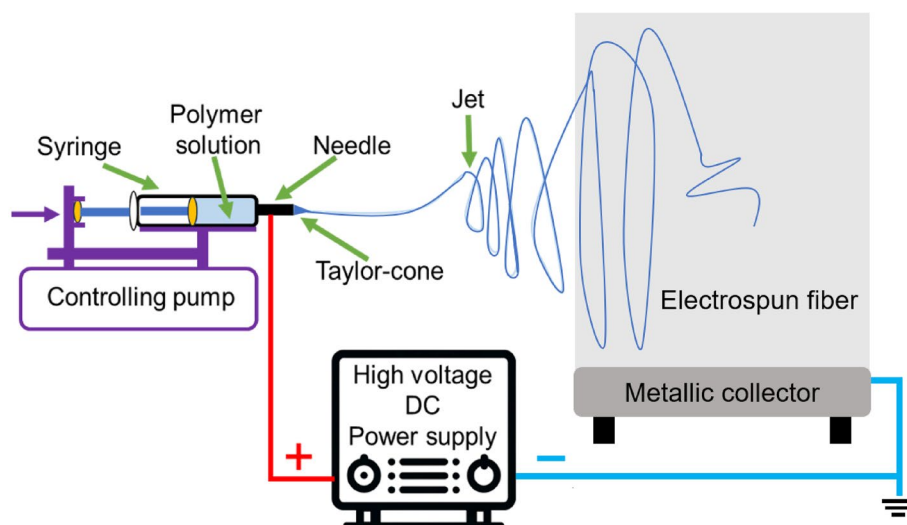


**FIGURE 2** | Schematic diagram of the basic ES set-up.

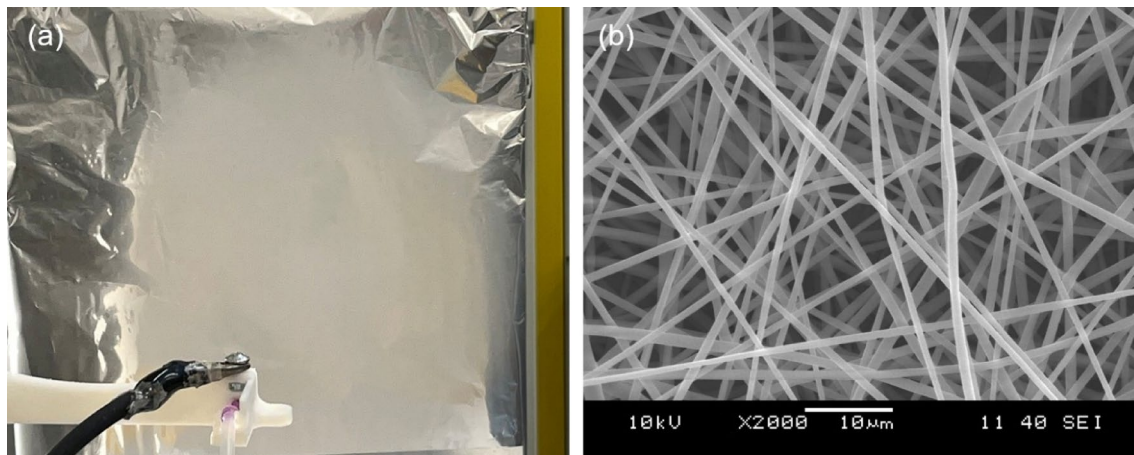


**FIGURE 3** | Electrospun nanofiber mat (a) on aluminum foil collector, and (b) magnification image by scanning electron microscopy (SEM).

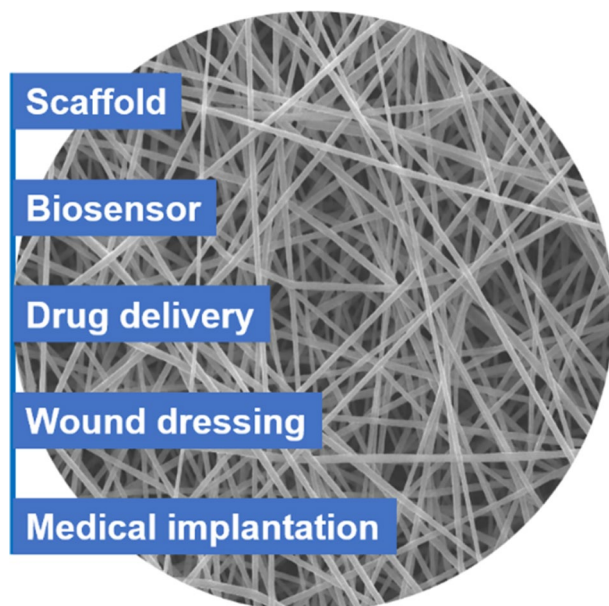


**FIGURE 4** | Applications of electrospun fibers in the medical field.

The basic ES setup mainly consists of a high direct current (DC) voltage power supply, a spinneret that is a metal capillary, and a collector, as shown in Figure 2. A semi-dilute polymer solution is loaded into a syringe and pressurized through the capillary at a constant flow rate [26, 27]. A semi-dilute polymer solution provides the right combination of viscosity, chain interactions, and force balance necessary for stable jet formation in the process, enabling the effective production of continuous fibers [28, 29].

Subsequently, a liquid droplet forms at the needle's tip [30]. The electrostatic field generates a force that opposes the surface tension of the liquid [31]. Because of the same electrostatic charges distributed along the surface of the conducting droplet, the droplet undergoes deformation, and upon reaching a particular conical shape, a liquid stream forcefully ejects from the surface [31, 32]. As the jet advances toward the collector, the solvent evaporates, leading to the formation of the fiber on the grounded collector [33], as shown in Figure 3. The principles and details of ES are summarized in [34] which we recommend for further reading.

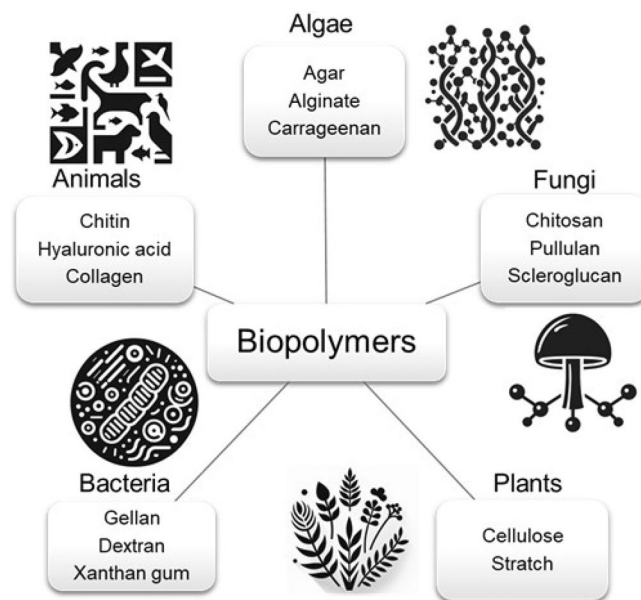


**FIGURE 5** | Potential natural origins of biopolymers. This figure is based on the work by R. Dimri et al., titled *Role of microalgae as a sustainable alternative of biopolymers and its application in industries*, and is licensed under the Creative Commons Attribution 4.0 International License (CC BY 4.0). The original work can be found in reference [38].

Presently, the significance of employing biopolymer electrospun nanofibers is notably pronounced across diverse fields within medical applications, as shown in Figure 4. Thus, electrospun nanofibers produced from biopolymers are extensively used in biomedical fields [35] because of their high specific surface area, high porosity, good adsorption capabilities, veil-like flexible structure, and versatility [36, 37].

## 2.1 | Biopolymers

ES is the most popular way to produce nanofibers from biopolymers in academia and industry. Subsequently, electrospun nanofibers produced from biopolymers are extensively used in biomedical fields such as TE and drug delivery [36, 37]. The potential natural origins for medical and engineering applications are shown in Figure 5.

Biopolymers such as poly(caprolactone) (PCL), poly(ethylene glycol) (PEG), poly(lactic acid) (PLA), poly(lactic-co-glycolic acid) (PLGA), chitosan, and gelatin are commonly engaged in ES for TE because of their excellent biocompatibility, capacity for biodegradation within the human body [39, 40], but they have different mechanical properties as shown in Figure 6. PLA offers high tensile strength and rigidity, making it ideal for structural integrity applications. In contrast, PEG is flexible and soft, which can be good for cell interactions but may not provide enough support. PLGA balances strength and flexibility, making it versatile for various uses. Gelatin is flexible and friendly to cells but lacks synthetic polymers' strength. Chitosan has low modulus, but it can be made stronger with cross-linking, while PCL is elastic and durable, allowing for fibers that can last longer. These differences allow for tailored electrospun fibers to meet specific functional requirements in various applications.

## 2.2 | Biocompatible Properties of Biopolymers

Biopolymers are polymers derived from natural sources, such as living organisms or renewable materials, often rendering them biocompatible properties [52]. Biocompatible polymers are specially engineered materials that do not trigger adverse reactions or toxicity when interacting with living tissues, cells, or organisms [53]. Subsequently, they comprise monomeric units which are similar to those found in living organisms and are often biodegradable [54]. Because these monomeric units are familiar to living organisms (i.e., amino acids in proteins, nucleotides in nucleic acids, and sugars in polysaccharides), they can be effectively recognized and broken down by enzymes. Furthermore, selecting biopolymers requires careful consideration of several critical factors, including mechanical properties, degradation rate, and appropriateness for specific tissues or organs [55, 56].

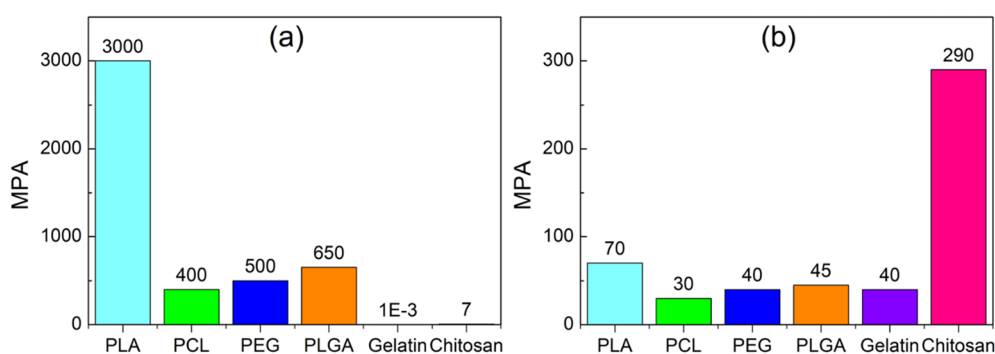


**FIGURE 6** | Mechanical behavior of biopolymer (a) Young's modulus; (b) Tensile strength. references: PLA [41, 42], PCL [43–45], PEG [46], PLGA [47–49], gelatin [47–49], and chitosan [50, 51].

**TABLE 1** | Degradation mechanisms and rates of major biopolymers.

Biopolymer	Primary degradation mechanism	Degradation rate (in vivo)	Degradation rate (in vitro)	Key factors influencing degradation	References
PLA	Hydrolysis, enzymatic	Months to years	Months to years	Molecular weight, crystallinity, pH, and temperature	[57, 58]
PCL	Hydrolysis	Months to years	Months to years	Molecular weight, crystallinity, and porosity	[59, 60]
PEG	Hydrolysis	Days to weeks	Weeks to months	Molecular weight and concentration	[61, 62]
PLGA	Hydrolysis	Weeks to months	Weeks to months (faster than in vivo)	Lactic-to-glycolic ratio, pH, and molecular weight	[63, 64]
Gelatin	Enzymatic	Days to weeks	Days to weeks	Cross-linking density and enzyme availability	[65]
Chitosan	Enzymatic, hydrolysis	Weeks to months	Weeks to months	Degree of deacetylation and molecular weight	[65]



**TABLE 2** | Parameters controlling electrospun fiber morphology and diameter in the case of biopolymers.

Parameters		Effect on fiber morphology	Biopolymer used
1. Solution parameters	Viscosity	Increasing viscosity will result in a greater fiber diameter. However, if the concentration of the polymer solution is low, continuous fiber structures cannot be created.	Chitosan [84], PLA [85], and gelatin [86]
	Polymer concentration	By increasing the polymer concentration, the fiber diameter increases.	PCL [87], PLGA [88] and PLA [89]
	The molecular weight of the polymer	Increasing the molecular weight leads to a decrease in beads on the fiber.	Chitosan [90], and PLA [91]
	Electrical conductivity	Rising electrical conductivity leads to a reduction in fiber diameter.	PLA [92] and PCL [93]
	Surface tension	Lowering the solution's surface tension results in smoother fibers.	Gelatin [94] and PLGA [95]
2. Process parameters	Applied voltage	An increase in applied voltage results in reduced fiber diameter.	Chitosan [96] and PCL [97]
	Distance from needle to collector	Reducing the gap between the needle and the collector results in the production of thinner fibers. However, if this gap becomes too small, the polymer jets may not have enough time to solidify, which can lead to the formation of beads on the fibers.	PCL [98] and chitosan [99]
	Feeding rate	By increasing the feeding rate, the diameter of the fiber increases.	PLGA [100] and PCL [101]
	Needle diameter	Higher needle diameter results in uniform fiber size distribution.	Chitosan [102]
3. Ambient parameters	Temperature	Increasing the temperature leads to increased fiber thickness because of faster evaporation.	PCL [103]
	Humidity	Increasing humidity causes an increase in the diameter and distribution of the pores.	PLA [104]

Several researchers have documented the degradation rates of various biopolymers under different conditions and timeframes. Biopolymer degradation may occur via mechanisms like hydrolysis, enzymatic, oxidative, or physical breakdown. To provide a clearer comparison, Table 1 summarizes the primary degradation mechanisms, rates, and influencing factors for commonly used biopolymers in various applications. Besides all these requirements, even the degradation products must be biocompatible.

The selection of these biopolymers is based on their mechanical, chemical, and biological properties, which influence their compatibility with cell development and determine their suitability for various applications. PCL is compatible with various cells, including osteoblasts and fibroblasts, making it ideal for bone regeneration and wound healing [66]. PLA has high tensile strength but is less effective for cell attachment, hence it is typically used in orthopedic implants and sutures [67]. PEG, while not as effective for cell attachment, is widely used for drug

delivery and cell encapsulation in tissue engineering [68]. PLGA supports fibroblasts and mesenchymal stem cells, making it a good choice for bone and cartilage regeneration and drug delivery [69]. Chitosan is excellent for promoting cell adhesion, particularly for cartilage and skin cells, and is often used in wound healing and cartilage repair [70]. Gelatin, which degrades quickly, supports a wide range of cells and is commonly used in soft tissue engineering and drug delivery [71]. These biopolymers are chosen for specific applications based on their ability to support cell development. Considering the degradation mechanisms of biopolymers, PLA and PCL are widely preferred for biomedical applications because they have predictable degradation rates and are biocompatible.

Based on research findings of Katila et al. [72] and Anderson et al. [73] PLA undergoes natural environmental degradation, breaking down into carbon dioxide (CO<sub>2</sub>) and water (H<sub>2</sub>O), contributing to its degradability. PLA readily undergoes hydrolysis within living organisms, producing lactic acid (LA), which can

be enzymatically degraded within the body, thus enhancing biocompatibility [74]. Furthermore, Gautam et al. [75] have studied an electrospun scaffold containing PCL, gelatin, and chitosan for TE. In this blend, they found that PCL is biodegradable, biocompatible, with strong mechanical stability, and helpful for TE utilities.

Furthermore, electrospun biopolymer nanofibers undergo a degradation process over time, leading to their breakdown. The elements influencing the degradation rates of biopolymers center around the conditions (in vivo or in vitro), material properties, including molecular weight and distribution [76], the degree of crystallinity [77], porosity and pore size, shape, and morphology [78], and polymer composition [79].

### 2.3 | Biomimetic ECM Scaffolds Using Electrospun Biopolymer Nanofibers

In the past few years, the use of electrospun biopolymers to emulate the ECM structure of bone tissue has gained greater importance in various scientific areas [80]. Since electrospun nanofibers possess a high surface-to-volume ratio and intricate porosity with good pore connectivity, they offer valuable attributes for advanced biomedical applications [81]. This can be accomplished by arranging the nanofibers into preferred configurations through layering or weaving [82]. The fibers can resemble the fibrous structure of the ECM.

The morphology of electrospun fibers is critical to generating fiber structures with favorable characteristics [83]. There are basically three types of parameters that affect the process: (1) solution-related, (2) process-related, and (3) ambient parameters. Their effect is summarized in Table 2 for various biopolymers.

A wide variety of materials can be used for the ES of ECM scaffolds. These are typically two-dimensional (2D), planar textile structures that need to be processed further to get the desired shape and properties [13]. Nonetheless, the ES technique has some limitations, including fibers with poor mechanical characteristics [105], a high residual solvent content [106, 107], the process is slow [39], and the difficulty in shaping custom forms of ECM structure [108]. Thus, electrospun materials are mainly suitable for applications that require a significant surface area, such as those in medical and filtration fields [109].

Building 3D structures through ES is quite challenging, leading some researchers to use multiple layers of electrospun mats to increase the material's thickness. Han et al. [110] were able to design an ECM structure by sequentially layering electrospun fibers three times to form three distinct layers, as shown in Figure 7. They obtained those different mat layers by modifying the rheological parameters of ES (as mentioned in Table 1). The first layer consisted of a dense, flat mat structure of electrospun material forming the bottom layer. Before making the middle layer, they introduced a digitated copper wire template with 300- $\mu\text{m}$  coils and 1 mm gaps to introduce porosity between the first and second layers. Subsequently, they fabricated middle and top layers intermediate between dense and loose structures. The connection between the middle and top layers was maintained at regularly spaced intervals, with large pores in between.

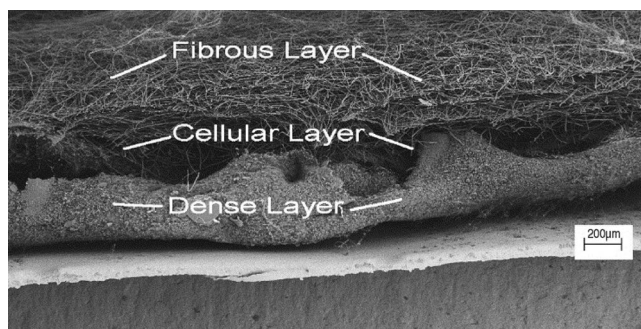


**FIGURE 7** | SEM image of the multilayer structured scaffold from the ES technique [110]. Reproduced with permission from Elsevier.

Overall, they created a simple 3D structure from electrospun fiber mats that could potentially replace ECM structures. Consequently, controlling the alignment and pattern of fibers within a scaffold can replicate the organized system of the ECM found in various tissues. Additionally, fibers can be treated with bioactive compounds like growth factors or signaling peptides, delivering chemical signals to cells and resembling the natural signaling molecules in the ECM [111]. Mao et al. [112] developed multilayer nanofibrous membranes from PLLA, stromal cell-derived factor-1 $\alpha$  (SDF-1 $\alpha$ ), and mesenchymal transition factor 01 (MT01). They employed a micro-sol ES technique to fabricate the individual nanofibrous layers of the scaffold. These layers were then stacked manually to create the multilayer structure necessary for the dual-delivery system. This scaffold served as a dual-delivery system to improve bone healing. It was designed to quickly release SDF-1 $\alpha$  to help mesenchymal stem cells (MSCs) move to the injury site while gradually releasing MT01 to encourage these cells to develop into bone cells through a specific signaling pathway mitogen-activated protein kinase. The study found that this approach improved the movement and bone-forming ability of MSCs in lab tests. Additionally, tests on rats with skull defects showed that the scaffold led to better bone growth and blood vessel formation, suggesting it could be a promising solution for treating bone injuries by imitating the body's natural healing processes.

Abudula et al. [113] created a composite scaffold for vascular TE through ES, reinforcing a matrix consisting of PLA and poly (butylene succinate) (PBS) with cellulose nano-fibrils (CNFs). To create composite fibrous scaffolds incorporating CNF (cellulose nanofiber), they first produced CNF/PBS composites with various concentrations using melt extrusion. Afterward, they dissolved a mixture of PLA and CNF/PBS composite in a chloroform and acetone solvent system with a 3:1 volume ratio, making fiber mats through ES.

PBS, as shown in Figure 8c,d, exhibited superior cell attachment when compared with PLA alone, as shown in Figure 8a,b. However, the PLA/PBS scaffold displayed notably better cell attachment performance than either PLA or PBS individually, as shown in Figure 8e,f. This improvement can be attributed to the scaffold's uniform fibrous structure, enhanced protein adsorption capacity, and moderately hydrophilic wetting properties [113]. Nonetheless, this study's limitations include the 2D structure, high solvent content, slow processing, and difficulty customizing scaffolds that cannot replace ECM scaffolds.

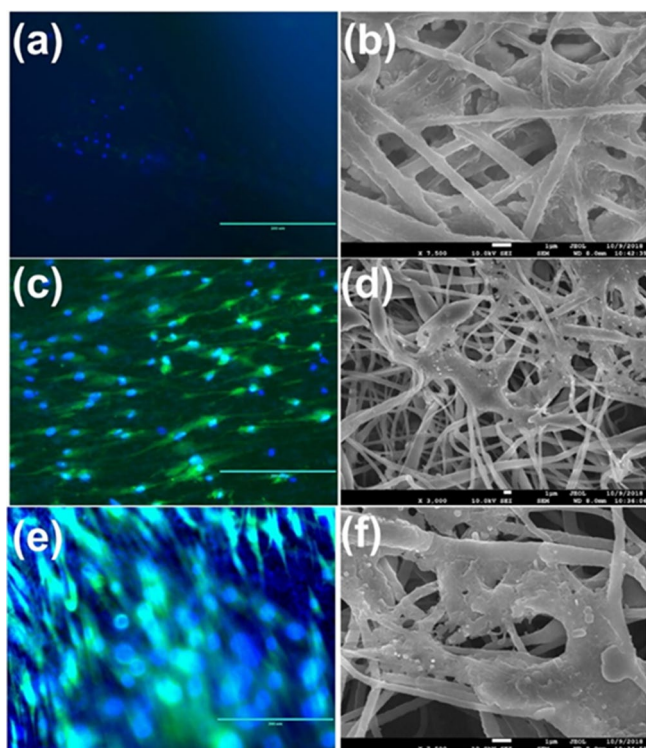


**FIGURE 8** | Images using green fluorescence protein (GFP) fusion protein and 4',6-diamidino-2-phenylindole (DAPI) GFP/DAPI and SEM of PLA (a, b), PBS (c, d), PLA/PBS (50/50) (e, f), and C4 composite scaffold [113]. Reproduced with permission from Springer Nature.

## 2.4 | Electrospun Fiber Sponges and Their Applications in 3D ECM Scaffolds

Electrospun fiber sponges are practical and suitable resources in TE, filtration, and drug delivery because of their porous 3D structure. They have greater porosity, closely resemble the ECM structure, and provide a more favorable microenvironment for cell growth, proliferation, and differentiation [114]. The principles and details of the techniques are summarized in reference [115].

The process of preparing electrospun short fiber sponge scaffolds is shown in Figure 9. These electrospun fibers are then collected and cut into short lengths, dispersing them in a container as shown. Subsequently, these dispersed fibers can be molded into various 3D shapes and sizes. The final product is a 3D electrospun fibrous sponge, which achieves its structure from the entanglement [117].

Moreover, Zhang et al. [118] created a scaffold by combining fish collagen/PLA nanofibers made through ES. First, nanofibers were dispersed in tert-butanol. Subsequently, they used a high-speed homogenizer to break down these nanofiber pieces uniformly and freeze-dried them to produce porous electrospun short nanofibrous sponges. These sponges contained various randomly arranged short fibers closely resembling the natural ECM structure. This arrangement facilitated cell adhesion and growth by speeding up the formation of new blood vessels at the sites of defects and controlling the process of bone marrow mesenchymal stem cells differentiating into bone-forming cells.

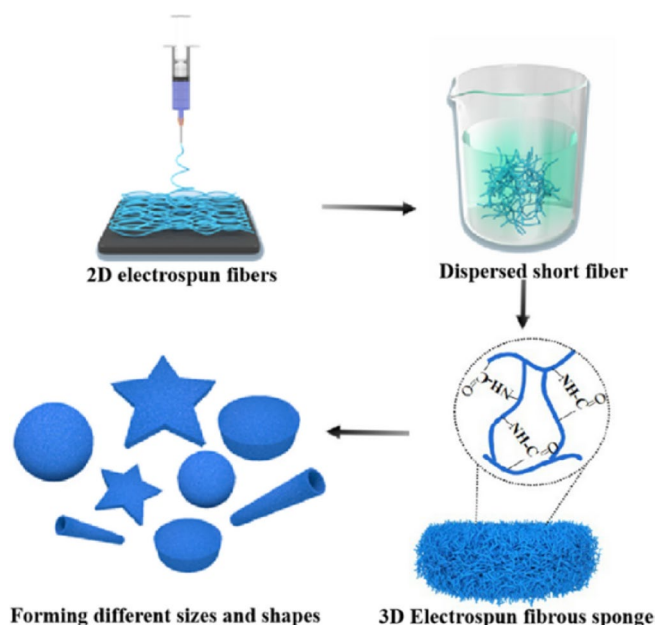


**FIGURE 9** | Simple illustration outlining the production process of electrospun short fiber sponge scaffolds. This figure is based on the work by Y. Li et al., titled Electrospun fibrous sponge via short fiber for mimicking 3D ECM, and is licensed under the Creative Commons Attribution 4.0 International License (CC BY 4.0). The original work can be found in reference [116].

**FIGURE 9** | Simple illustration outlining the production process of electrospun short fiber sponge scaffolds. This figure is based on the work by Y. Li et al., titled Electrospun fibrous sponge via short fiber for mimicking 3D ECM, and is licensed under the Creative Commons Attribution 4.0 International License (CC BY 4.0). The original work can be found in reference [116].

## 3 | Three-Dimensional (3D) Printing Technique

The 3D printing is a manufacturing technique that builds objects layer-by-layer, using a 3D computer-aided design (CAD) model [119–121]. Multiple investigations have demonstrated that 3D printing is promising in enabling precise control over individual 3D geometries [122] and creating scaffold structures with considerable pores [123]. 3D printing offers extreme customization options and operates efficiently, leading to widespread adoption, particularly in medical fields [124]. Additionally, 3D printing includes a range of different types, each designed for different uses.

### 3.1 | Different Types of 3D Printing Techniques

Various 3D printing techniques are used for 3D printing scaffolds, among which the most popular ones are fused filament fabrication (FFF), stereolithography (SLA), and selective laser sintering (SLS), as shown in Figure 10.

Each technique has advantages and disadvantages when making an ECM scaffold. We briefly summarized those in Table 3. The main obstacle in the 3D printing of scaffolds is achieving the desired porosity because the finest resolution possible is typically in the microscale, which is still too large for most cells to attach to the scaffold's surface [128].

As mentioned previously, ECM comprises a dynamic arrangement of proteins, glycoproteins, and various molecules, creating a complex microenvironment crucial in influencing cell behavior and tissue function. Therefore, extreme diffusivity is also necessary for 3D scaffolds to promote the efficient transport of



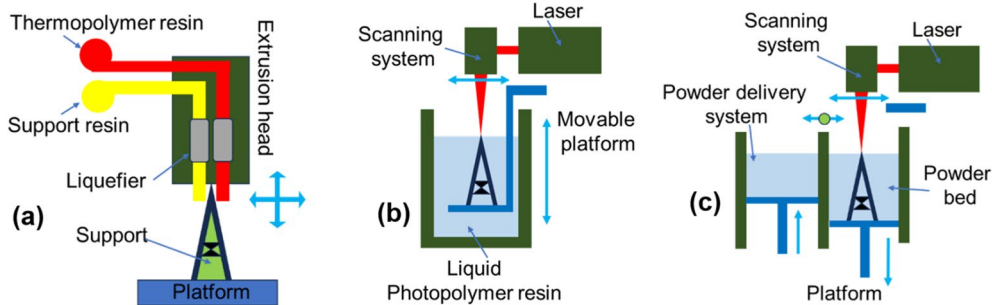


**FIGURE 10** | Common 3D printing methods for scaffold fabrication (a) Fused filament fabrication (FFF), (b) Stereolithography (SLA), and (c) Selective laser sintering (SLS). This figure is based on the work by Z.-X. Low et al., titled *Perspective on 3D printing of separation membranes and comparison to related unconventional fabrication techniques*, and is licensed under the Creative Commons Attribution 4.0 International License (CC BY 4.0). The original work can be found in reference [125].

**TABLE 3** | Advantages and disadvantages of the three main types of 3D printing used for creating ECM structures.

3D printing type	Advantages	Disadvantages	References
FFF	Cost-effective, wide material selection, simple setup, and operation	Lower resolution, visible layer lines, and limited precision	[126, 127]
SLA	High resolution, wide material selection, and precise features	Expensive equipment and materials, and post-processing requirements	[126, 127]
SLS	High strength and durability, material versatility, and complex geometries	High equipment and material costs, limited surface finish, and longer production times	[126, 127]

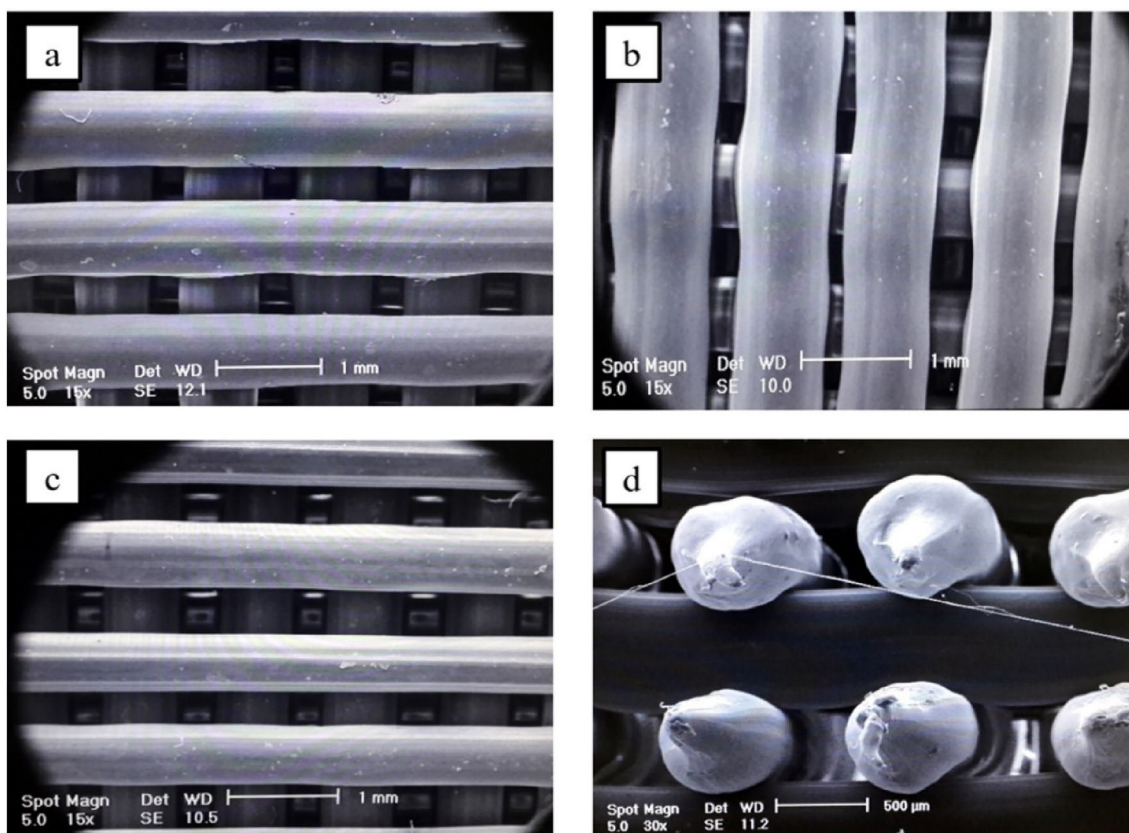


**FIGURE 11** | FFF technique to create 3D PLA scaffold structures [132]. Reproduced with permission from Elsevier.



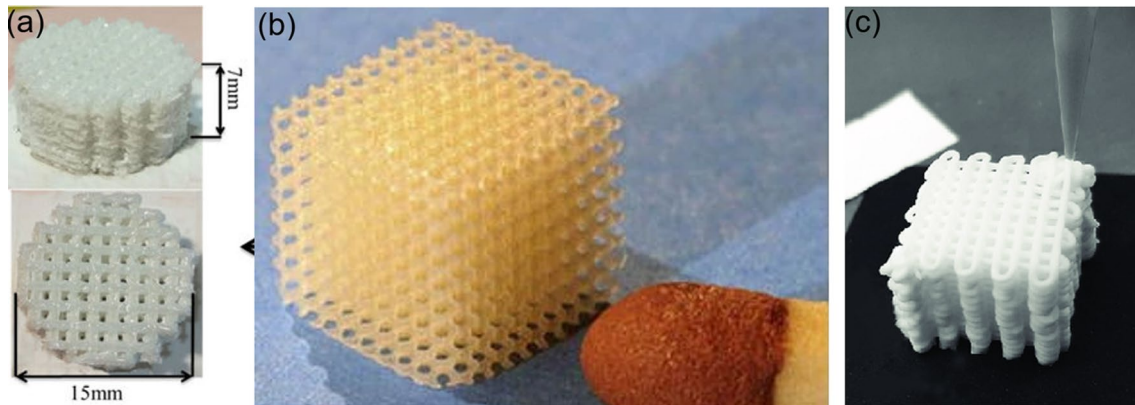


**FIGURE 12** | ECM structure made from 3D printing (a) SLS technique [133], (b) SLA technique [134], and (c) FFF. Those figures are licensed under the Creative Commons Attribution 4.0 International License (CC BY 4.0).

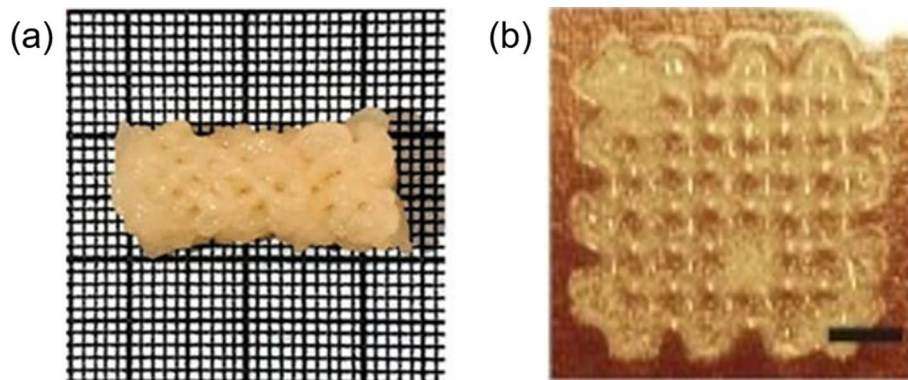


**FIGURE 13** | Schematic representation of 3D bio-printed scaffolds used in TE (a) a clavicle bone scaffold created using GelMA-based bioink [139]. Reproduced with permission from John Wiley and Sons. (b) a scaffold made of methacrylated hyaluronic acid. This figure is based on the work by Michelle T. Poldervaart et al., titled *3D bioprinting of methacrylated hyaluronic acid (MeHA) hydrogel with intrinsic osteogenicity* and is licensed under the Creative Commons Attribution 4.0 International License (CC BY 4.0). The original work can be found in reference [140].

oxygen and nutrients, and the size of pores is one of the main factors in cell distribution and the penetration of nutrients. Nonetheless, achieving better dimensional accuracy requires adding more layers, which slows down the process. This challenge means that 3D printing may not be as practical as traditional mass-production methods like extrusion or injection molding [129]. However, there are many areas for improvement in 3D printing, such as the stringing that occurs in FFF techniques when small strands of melted filament stretch between parts of the print. Retraction pulls filament back into the nozzle during movement. Over-extrusion results in excess material on the print's surface, leading to a rough texture and visible spots.

The FFF technique operates by extruding continuous filament, enabling the customization of parameters such as layer thickness, orientation, and pore structure [130, 131]. On the other hand, it uses high temperatures to melt the thermoplastic filament, and it is not capable of processing tiny details or pores. A sample of a 3D structure that is quite typical for FFF printing is shown in Figure 11.

SLS and SLA are sophisticated 3D printing methods that use lasers to build objects, but they operate differently. SLS uses a laser to melt and fuse layers of thermoplastic powder, which supports complex shapes and eliminates the need for additional support structures, resulting in strong and durable

parts. In contrast, SLA is an earlier rapid prototyping technique that employs UV light to solidify a liquid polymer layer by layer. Once a layer hardens, the printer proceeds to the next, gradually building up the model. This method offers extremely high detail and precision, making it ideal for intricate designs. Both technologies ensure excellent dimensional accuracy, samples of scaffolds produced by each 3D printing technique are depicted in Figure 12. The principles and details of these techniques are well-summarized in [126, 135] which we recommend for further reading. Besides the three main 3D printing methods for creating ECM scaffolds, there are other, less commonly used techniques like selective laser melting, photolithography, soft lithography, and digital light processing [127, 136–138].

### 3.2 | Bioprinting

Among the various 3D printing methods, bioprinting is a subfield that focuses on creating living biological constructs. Bioink printing entails layering cell-containing biomaterials, termed bioinks, to fabricate 3D structures resembling natural tissues, as shown in Figure 13. Bioprinting creates scaffolds by layering bioinks containing cells and materials like alginate or collagen [141]. Unlike the FFF 3D printing technique, which melts plastic with heat, bioprinting typically works at room

temperature and uses chemical processes to solidify the scaffold [142]. Subsequently, bioprinting creates an ideal environment for cells within ECM scaffolds, allowing precise control over their organization and structure.

Subsequent stabilization via crosslinking or gelation fosters cell survival, growth, and specialization within the printed constructs. Bioprinting finds wide application possibilities in TE, enabling the incorporation of ECM components into printed tissues for various purposes [143]. Various advances and developments in bioprinting for emulating ECM structures include bio-ink [144], multi-material printing [145], cell-laden constructs [146], vascularization [147], and biofabrication techniques [148]. Their main application possibilities are shown in Table 4.

The bioinks often combine synthetic and natural materials, such as hydrogels, fibrin, collagen, and hyaluronic acid, to replicate the ECM's mechanical and biochemical properties [156]. Shin and Kang [157] created gelatin bioinks for 3D printing, finding them suitable for precise cell placement in 3D structures. Furthermore, their research demonstrated the bioink's ability to accurately position different cell types within 3D arrangements. The principles and details of the techniques are summarized in reference [158].

Even though bioprinting can create structures with various shapes and use different materials, it is still difficult to precisely reproduce the detailed nanoscale features and complex makeup of bone ECM scaffolds. The layered structure of bone ECM includes nanoscale mineralized collagen fibers, which makes it challenging for current bioprinting methods to achieve the same precision and complexity as natural ECM scaffolds.

#### 4 | Synergistic Approaches Between 3D Printing and ES Techniques

Recent advances in TE have improved electrospun materials, leading to the creation of complex ECM with multiscale hierarchical scaffolds by combining ES with 3D printing techniques. This chapter explores the latest methods for making these hybrid ECM scaffolds and how their micro- and nano-scale features affect cell behavior like attachment, migration, and differentiation.

#### 4.1 | Challenges in Replicating Natural ECM Structure in 3D-Printed Scaffolds

Typically, 3D-printed ECM scaffolds by FFF techniques do not offer a satisfactory cell adhesion environment because of the formation of too large pores [159]. These characteristics deviate from the natural ECM structure and fail to provide suitable surfaces for effective cell adhesion. Moreover, collagen and elastin within the ECM are characterized by their fibrous nature, with diameters typically falling in the range of about 50–500 nm. These dimensions are significantly smaller than what can be achieved in 3D-printed scaffolds, making it challenging for them to establish attachment [160–163]. Murphy and O'Brien [164] showed that the size of pores in random ECM scaffolds varies from around 100–500  $\mu\text{m}$ . However, cell clusters were observed at the edges of the scaffolds with reduced pore sizes ranging from 85 to 120  $\mu\text{m}$ , which restricted the penetration of cells into the scaffold.

Therefore, enhancing the effectiveness of 3D-printed ECM scaffolds is essential to create a microenvironment that closely simulates natural conditions.

#### 4.2 | Enhancing 3D-Printed Scaffolds With ES

The combination of both ES and 3D printing techniques amplifies their advances in constructing complex structures like ECM scaffolds, as shown in Figure 14. They enhance each other's capabilities and address their limitations. As previously noted, designing a 3D-printed ECM scaffold involves a detailed process considering tissue type, mechanical properties, porosity, and biodegradability [166, 167]. Specific porosity and pore size are crucial for bone scaffolds to support cell infiltration and nutrient distribution. Therefore, this integration of ES and 3D printing thus forms a potent combination for creating advanced biomimetic scaffolds.

In essence, integrating ES and 3D printing techniques improves the precision in creating intricate structures that closely resemble natural ECM tissues, offering better support for cell organization and adhesion [168]. Combining both methods must create a suitable microenvironment, provide mechanical support, and control cell activities [169–172]. Nanofibrous networks provide a substantially larger surface area than dense materials, allowing cells to encounter additional adhesion

**TABLE 4** | The application of bioprinting for constructing ECM structures.

Categories	Function	Reference
Tissue engineering	Offer a framework for cells to adhere to and arrange themselves within.	[149]
Cell encapsulation	Enables accurate positioning of cells within a 3D framework, facilitating the setup of cells within an environment that closely mimics the natural ECM.	[150]
Bioactive components	Permits tailoring the ECM structure to align with the tissue being addressed.	[151]
Customized ECM	Enables the adaptation of the ECM structure to correspond with the specific tissue being focused on.	[152, 153]
Regenerative medicine	It can produce tissue grafts or implants that include ECM components, promoting tissue repair, and regeneration.	[154, 155]

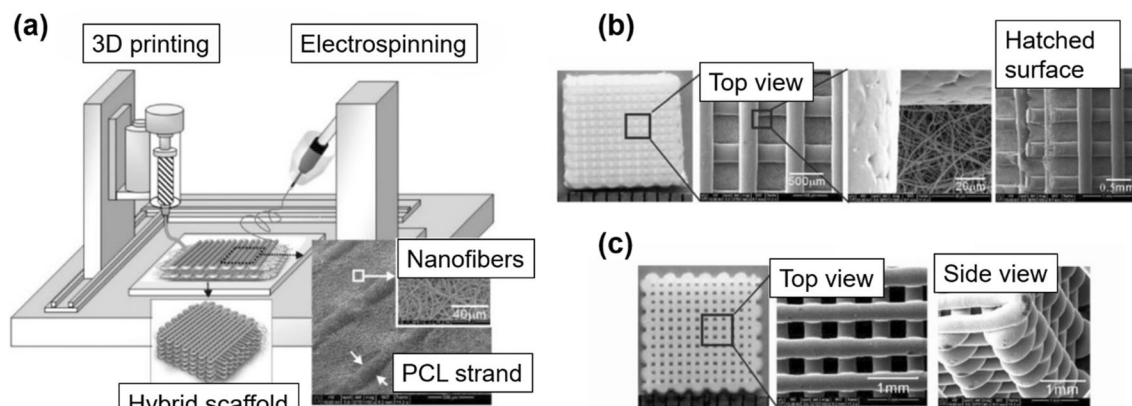


**FIGURE 14** | (a) Schematic diagram illustrating the combination of ES and 3D printing techniques for creating ECM scaffold, (b) SEM images of hierarchical PCL scaffolds produced by integrating ES with 3D printing. (c) SEM images of PCL scaffolds were produced exclusively by the 3D printing technique [165]. Reproduced with permission from John Wiley and Sons.

sites and promoting their spreading and directed movement [173]. Consequently, electrospun nanofibers can improve the 3D-printed ECM scaffolds and render them more biomimetic. Electrospun layers may also enhance the scaffold's structural reliability. The nanofibrous structure promotes cell adhesion and proliferation, helping cells to grow and differentiate into the desired tissue type [174, 175].

### 4.3 | Hybrid Fabrication Methods and Combination Approaches

There are several approaches to combining ES and 3D printing techniques to make a scaffold-like ECM. Each of these approaches can be tailored depending on the specific requirements of the TE application, such as the type of tissue being mimicked, desired mechanical properties, and biological functionality. We outlined several combination methods in Table 5, focusing on their approaches, benefits, and potential applications.

One effective way to combine these two techniques is using multilayered designs, where electrospun mats are placed over 3D-printed substrates to create composite scaffolds with multiple scales [181]. Making a scaffold using a sequential fabrication approach involves either layer-by-layer or post-printing ES methods. In the first method, layers of electrospun fibers are deposited alternately with 3D-printed structures. This can be done by using two separate setups: one for ES and one for 3D printing, where the substrate is moved between the two during the fabrication process, as illustrated in Figure 15. On the other hand, in post-printing ES, the 3D-printed scaffold is first created, and then electrospun fibers are deposited onto or around the scaffold. While this approach combines the mechanical support of 3D-printed structures with the fibrillary mimicry of ECM provided by ES, it faces several challenges. Misalignment between the printed scaffold and the electrospun fiber mats often occurs, especially in manual layer-by-layer assembly, leading to inconsistencies in scaffold architecture. Additionally, weak interfacial bonding between the electrospun layers and the 3D-printed scaffold can

compromise mechanical integrity. The need for separate setups and transitions between processes further increases production time and complexity.

Recently, Cao et al. [183] developed a dual-scale PCL/nHA/MWCNTs scaffold for bone regeneration by combining ES with layer-by-layer 3D printing as shown in Figure 16. They dissolved PCL, nano-hydroxyapatite (nHA), and multi-walled carbon nanotubes (MWCNTs) to create composite scaffolds through 3D printing, which were then reinforced with an electrospun layer of the same material. This approach resulted in a dense, disordered layer of nanofibers tightly bonded to a porous 3D-printed scaffold, enhancing cell seeding, adhesion, and proliferation.

Another method to combine these two techniques is to print 3D grids and then apply electrospun nanofiber mats, securing the mats with adhesive. Recently, Belgheisi et al. [184] created hybrid scaffolds by sticking a PCL or layered double hydroxides (LDH) and PCL nanofiber mats between two 3D-printed two-layer grids. These mats were attached to 3D-printed circular PCL grids with 400 μm strands using a PCL-based glue made from a 15% PCL solution in a DCM/DMF mixture (2:1 v/v), applied at 20 spots/cm<sup>2</sup>. Adding LDH reduced the fiber diameter and increased the surface roughness of the mats. Structural analysis showed that the nanofiber mats adhered well to the grids without affecting their shape. The resulting LDH/PCL scaffolds had a higher Young's modulus and exhibited faster degradation. In vitro tests indicated better cell adhesion, increased alkaline phosphatase activity, and more calcium deposition, suggesting that these scaffolds are promising for bone TE because of their enhanced mechanical strength, bioactivity, and support for cell growth and mineralization.

Gonzalez-Pujana et al. [176] investigated hybrid scaffolds using 3D printing and ES to create semicrystalline PCL scaffolds. They produced these hybrid scaffolds by layering 10 layers of 3D-printed PCL filament with electrospun PCL solution, resulting in structures that were 21 mm in diameter and 1 mm in height. The 3D printer employed had a 0.4 mm nozzle, operated at 110°C, and used a printing speed of 30 mm/s with a 75% infill density and 100% flow rate.



TABLE 5 | different methods for integrating ES with 3D printing to develop ECM-like scaffolds.

Method	Description of approach	Key benefits	Ideal applications	Reference
Sequential fabrication	First, use 3D printing to create a structured scaffold. Then, apply ES to deposit nanofibrous layers on the scaffold.	It provides mechanical support with 3D printing and mimics the ECM fibrillary structure with ES.	Suitable for complex multi-layered tissues.	[176, 177]
Hybrid fabrication	Simultaneously uses 3D printing and ES in a single process to create composite structures.	Integrates the benefits of both techniques in one step, saving time and improving interfacial bonding between fibers and the printed matrix.	It is useful in orthopedic applications, where bone and soft tissue integration is necessary.	[178]
Coaxial printing	Implement a coaxial nozzle that can do both 3D printing and ES, allowing precise spatial deposition of materials.	Allows for precise control over material deposition, enabling the creation of graded scaffolds with varying properties.	Effective for creating scaffolds with zone-specific characteristics, like cartilage-to-bone transitions.	[179]
Post-processing functionalization	It starts with a 3D-printed scaffold that is subsequently enhanced by ES bioactive materials to increase functionality.	Enhances the bioactivity of the scaffold, promoting better cell attachment and growth.	It is particularly suitable for creating scaffolds that require enhanced cell responses for regeneration.	[180]

The scaffolds exhibited shape memory, had good mechanical properties, and featured a porous network with both micro- and macro-pores. SEM and Fourier transform infrared spectroscopy showed that the scaffold materials were well-integrated and free of residual solvents. The scaffolds demonstrated good flexibility and shape recovery and were hydrophobic enough to support cell culture. When MC3T3-E1 preosteoblasts were cultured on these scaffolds for 21 days, they showed increased growth, spreading, and osteogenic differentiation. These results suggest that the hybrid PCL scaffolds effectively support bone cell growth and differentiation for bone regeneration applications. Although this approach reduces time and enhances interfacial bonding, coordinating the two processes is technically challenging. Each method has specific requirements, such as certain voltage and flow rates, that must be balanced to achieve consistent results. The process is further constrained by equipment limitations and the need for specialized systems to integrate the methods. Additionally, material choices are restricted to those compatible with both processes.

In the context of bone regeneration, *in vivo* studies have shown that hybrid scaffolds effectively support the osteogenic differentiation of stem cells and promote vascularization for successful bone healing. For instance, research involving these scaffolds in animal models has reported enhanced bone formation rates compared with traditional scaffolds, with noticeable improvements in both the quality and quantity of bone growth [178, 185]. Recent research has also highlighted “osteoinductive or smart biomaterials,” which show great potential for helping with bone healing. These materials can interact with their environment and encourage new bone growth. However, the exact biological processes involved are still not fully understood, and more research is needed [186]. For instance, functionalization by post-processing enhances 3D-printed scaffolds with electrospun bioactive layers, improving cell attachment but often causing uneven fiber deposition or scaffold weakening. Similarly, coaxial printing combines 3D printing and ES for precise material placement, faces issues like clogging, and relies on costly, high-precision, specialized equipment.

#### 4.4 | Advanced Methods and Functionalization Techniques for ECM Scaffolds

Numerical studies highlighted the results and advantages of integrating those techniques to mimic ECM-like scaffolds, particularly focusing on promoting cell growth. After scaffold fabrication, the surfaces can be modified through ES bioactive substances or ECM components onto the 3D printed structure to enhance cell attachment and growth [187]. Cells, such as stem or tissue-specific cells, can be seeded onto electrospun scaffolds [188]. In addition, biomimetic factors such as hydroxyapatite or growth factors can be added through the electrospun fibers to enhance bone-like properties [189]. Growth factors like bone morphogenetic proteins (BMPs), vascular endothelial growth factor, and fibroblast growth factor are often used in hybrid ECM scaffolds [190]. For instance, BMPs trigger the proliferation and differentiation of osteoprogenitor cells and are commonly incorporated into bone scaffolds to enhance osteogenesis and stimulate bone formation and regeneration [191]. Bioactive peptides, such as the RGD (Arg-Gly-Asp) peptides, are commonly used

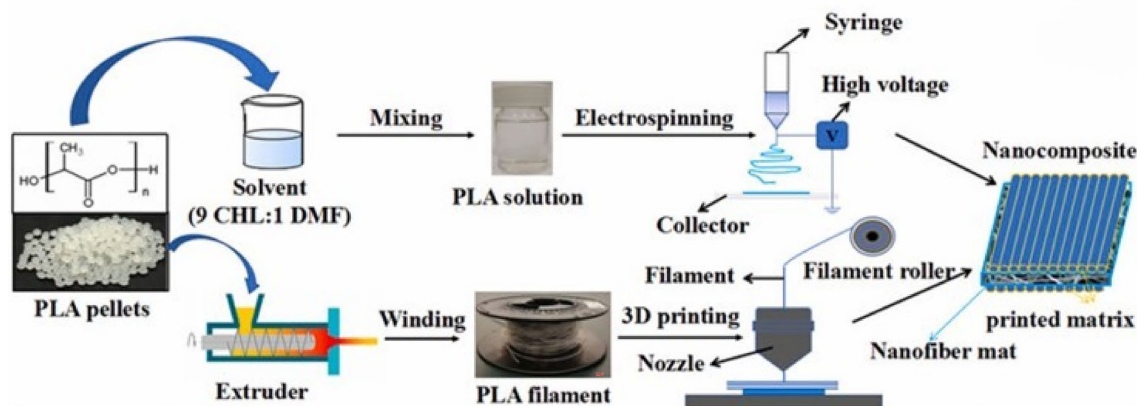


**FIGURE 15** | The preparation process of the 3D printed structure including the ES technique. This figure is based on the work by H. He, and K. Molnár, titled Fabrication of 3D printed nanocomposites with electrospun nanofiber interleaves, and is licensed under the Creative Commons Attribution 4.0 International License (CC BY-NC-ND 4.0). The original work can be found in reference [182].

to functionalize electrospun fibers [192]. These peptides mimic the cell-binding patterns found in natural ECM proteins. The inclusion of RGD peptides can improve osteogenic differentiation when used in bone scaffolds. However, adding bioactive molecules during fabrication must align with both processes. Rajzer et al. [193] electrospun gelatin and osteogenon nanofibers onto a PLLA scaffold. To improve the stability of the gelatin fibers in aqueous solutions, they were crosslinked using glutaraldehyde vapors. After 1 week in simulated body fluid, apatite crystals formed on the gelatin surface because of osteogenon mineralization. In addition, cells successfully adhered to and proliferated on the gelatin layer, demonstrating the biocompatibility of the composite scaffolds.

Rosales-Ibáñez et al. [194] designed a bioactive bilayer scaffold for ECM bone by modifying the surface of the scaffolds. They enhanced the scaffold with aminolysis and gelatin grafting. The scaffold was cleaned, treated with various solutions, and modified to improve cell adhesion. Additionally, the inner layer of the ECM scaffolds intended for slow degradation replicates the shape and structure needed for new tissue formation. Meanwhile, the outer layer degrades more quickly and promotes cell proliferation because of its porous nature and composition. The scaffold surface was improved through aminolysis and gelatin grafting, which led to better cell adhesion. Cytocompatibility tests revealed that electrospun/3D-printed scaffolds with gelatin significantly boosted cell proliferation compared with those without, facilitating the differentiation of human adipose stem cells (hASCs) into the osteogenic lineage, thus making these scaffolds suitable for mimicking ECM scaffold of bone.

Pore size and distribution are critical in hybrid scaffolds as they directly influence nutrient transport, cell adhesion, and tissue regeneration. Interconnected pores are particularly important, as they ensure efficient pathways for oxygen, nutrients, and cell migration [195]. Huang et al. [196] introduced a new hybrid printing method that combines screw-assisted additive manufacturing with rotational ES to create dual-scale scaffolds with aligned nanoscale fibers, as shown in Figure 17. The rotating drum was designed to manage the density and alignment of electrospun fibers. The process started with printing PCL using a 0°/90° orientation pattern and 350 μm square pores. This

scaffold was then positioned on a rotating ES collector, where varying the rotation speed helped to achieve better fiber alignment. As a result, the team successfully produced 3D-printed PCL structures with uniform microscale features and improved fiber alignment. Cells grown on these aligned nanofiber scaffolds displayed more elongated shapes and enhanced anisotropic organization.

Vyas et al. [197] created a dual-scale scaffold consisting of 3D-printed and electrospun PCL fibers using a screw-assisted extrusion 3D printer, as shown in Figure 18a. The parameters for this process included a deposition speed of 12 mm/s and a screw rate of 7.5 rpm. The 3D-printed fibers had a circular geometry with a diameter ranging from 287.2 to 27.5 μm and a pore size of 299.2–18.3 μm. Subsequently, electrospun fibers were deposited onto the scaffolds at specific layers, with a fiber diameter ranging from 820 to 56 nm, as shown in Figure 18b. Biological tests revealed that cells migrated and aligned with an elongated morphology within the pores of the printed microfibers, as shown in Figure 18c.

Gill et al. [198] developed a new approach to create a hybrid scaffold of ES and 3DP with varying laydown angles (0°, 30°, 45°, and 90°), which represent the angle between fibers in successive printed layers. After printing, human glioblastoma cells were seeded as aggregates on the scaffolds. The study found that all designs, except the 0° laydown angle, showed higher initial cell attachment, likely because the stacked fibers created more surface area. Additionally, the cells migrated outward from the aggregates, with their movement directed by the fiber alignment, following the path of the fibers. Paxton et al. [199] fabricated PCL scaffolds with aligned and non-aligned fibers at laydown angles of 20°, 50°, and 90°. The aligned scaffolds had fibers stacked precisely on top of each other with uniform pores (0.5 mm<sup>2</sup>), while the non-aligned scaffolds featured inconsistent fiber placement and varied pore sizes (0.02 mm<sup>2</sup>–0.33 mm<sup>2</sup>). MC3T3-E1 cells were seeded onto the scaffolds. Lower laydown angles (20° and 50°) led to uncontrolled cell bridging, whereas the 90° scaffolds showed cells growing along the fibers before closing the pores. In non-aligned scaffolds, cells initially filled smaller pores, but after 3 weeks, aligned scaffolds displayed more consistent growth and pore bridging as shown in Figure 19.

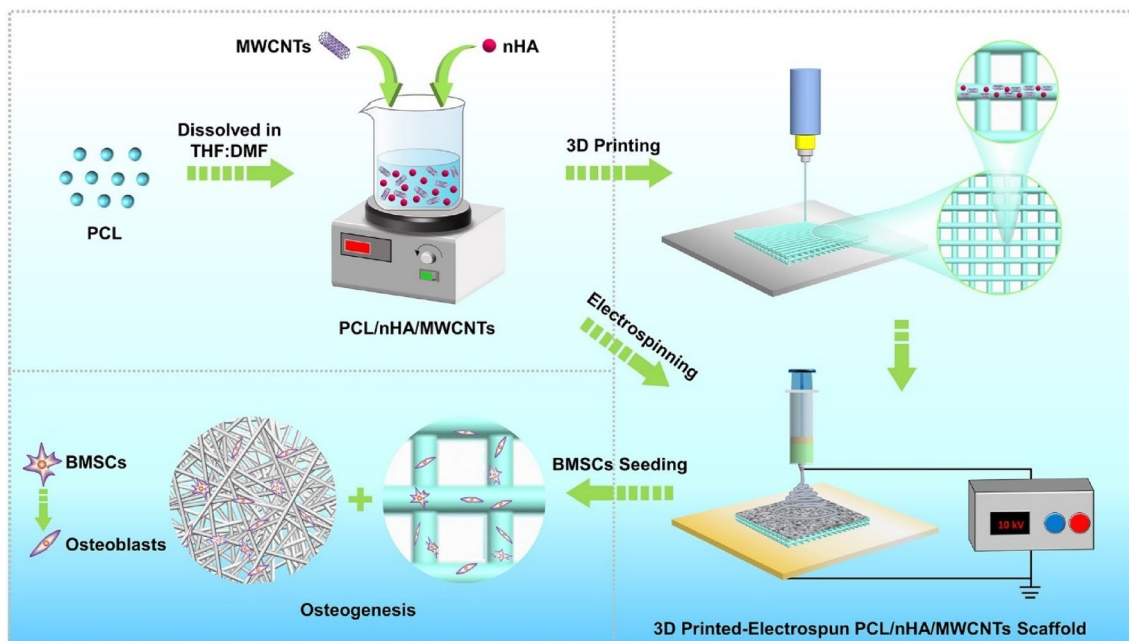


**FIGURE 16** | The integration of ES with layer-by-layer 3D printing to construct a 3D-printed PCL/nHA/MWCNTs scaffold for bone regeneration. This figure is based on the work by Cao et al., titled *3D printed-electrospun PCL/hydroxyapatite/MWCNTs scaffolds for the repair of subchondral bone* and is licensed under the Creative Commons Attribution 4.0 International License (CC BY 4.0). The original work can be found in reference [183].

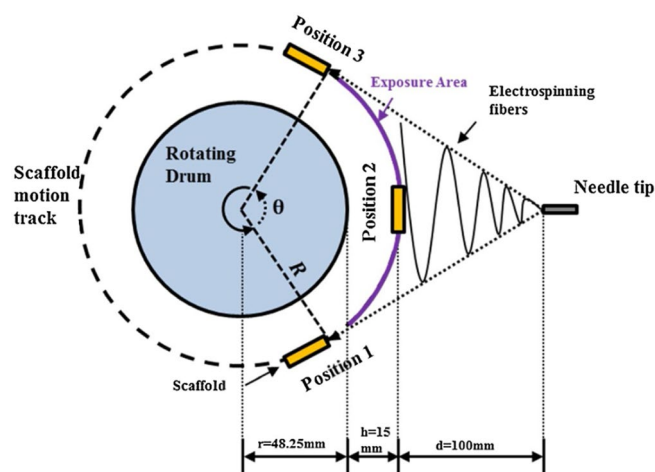


**FIGURE 17** | Hybrid printing technique that integrates screw-assisted 3D printing with rotational ES. This figure is based on the work by Huang et al., titled *Engineered dual-scale poly( $\epsilon$ -caprolactone) scaffolds using 3D printing and rotational electrospinning for bone tissue regeneration* and is licensed under the Creative Commons Attribution 4.0 International License (CC BY 4.0). The original work can be found in reference [196].

#### 4.5 | Electrospun Fiber Sponges in 3D Printing Technique

Electrospun nanofiber sponges are porous structures that enhance cell attachment, proliferation, and nutrient exchange. Various fibrous sponges have recently been developed by combining electrospun nanofibers with conventional hydrogels. This simple method combines electrospun fiber membranes into hydrogels to create composite fiber sponges

[200]. Integrating these sponges into 3D-printed structures combines the benefits of both techniques, resulting in improved mechanical properties and better control over scaffold architecture.

Yu et al. [201] demonstrated a solid 3D composite scaffold from PCL and gelatin by combining ES with 3D printing techniques. The process begins by cutting the electrospun PCL/gelatin nanofibers into small pieces ( $2 \times 2$  mm) using a high-speed dispersion homogenizer in a tert-butanol solution. Then, a PCL mesh scaffold is formed using 3D printing. In the third step, the dispersed PCL/gelatin nanofibers are inserted into the mesh of the PCL scaffold. After freezing for 24 h, the 3D composite scaffolds are placed in a 2.5% glutaraldehyde solution for 20 min, washed three times with deionized water, and freeze-dried again for 24 h. The microporous structure provided by electrospun fibers greatly enhanced cell proliferation and supported bone tissue repair applications. Moreover, electrospun nanofiber sponges can be integrated into the 3D-printed structure either during printing or through post-processing methods such as adhesive bonding. PGA-based electrospun nanofiber sponges have been applied in 3D-printed ECM structures. Kobayashi et al. [202] developed a unique PGA–collagen nanofiber sponge, achieving fast cellularization and neovascularization in a week, hinting at the possibility of bio-derived matter-free scaffold designs for complete cell population and vascularization.

Electrospun layers can serve as biomimetic interfaces, guiding cellular attachment and migration, while improving mechanical strength, especially when combined with 3D-printed hydrogels instead of thermoplastic polymers. For instance, Yoon et al. [203] used 3D bioprinting to create multilayered hybrid constructs by integrating PCL electrospun mats with



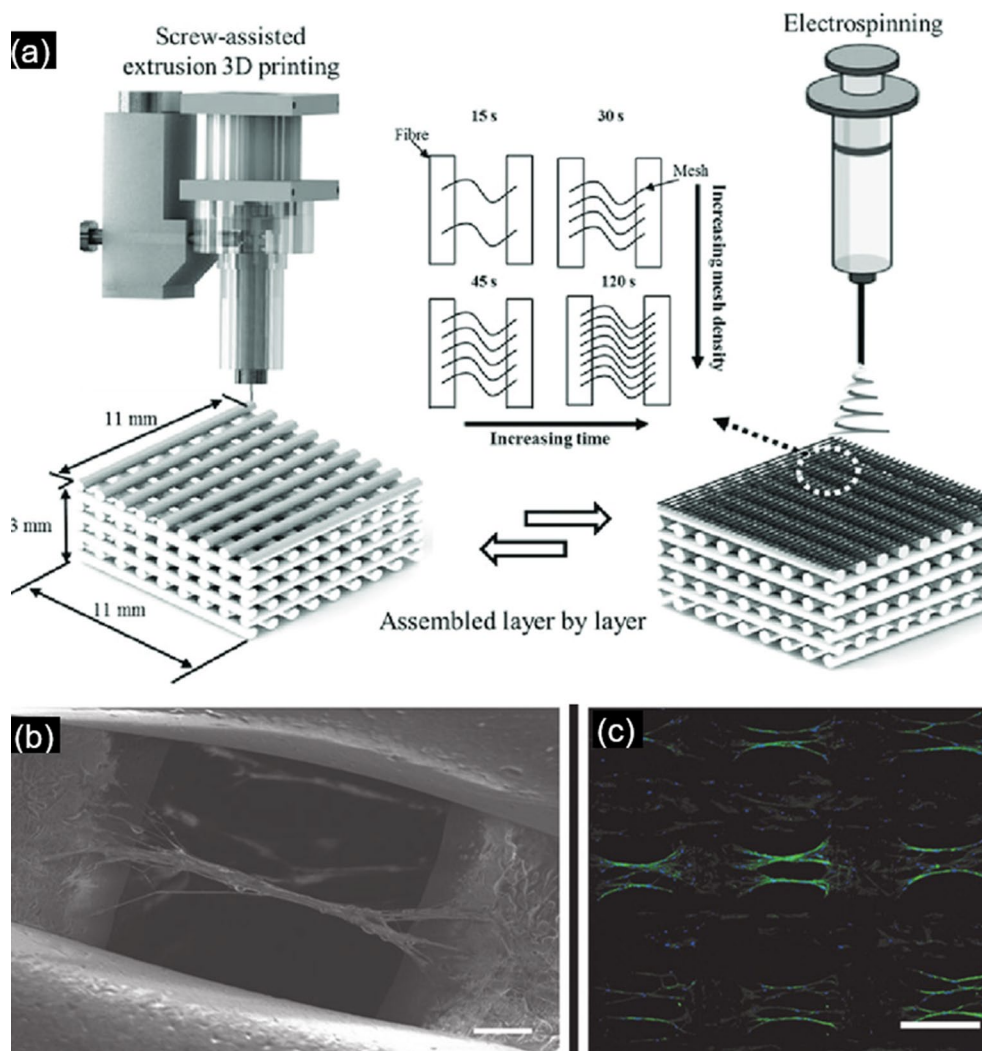


**FIGURE 18** | (a) Diagram illustrating the fabrication process of a dual-scale scaffold using both 3D printing and ES. (b) Pictures showing cells seeded onto the 3D-printed scaffold, (c) SEM image depicting cell alignment and bridging within the dual-scale scaffold. This figure is based on the work by C. Vyas et al., titled *Three-Dimensional Printing and Electrospinning Dual-Scale Polycaprolactone Scaffolds with Low-Density and Oriented Fibers to Promote Cell Alignment* and is licensed under the Creative Commons Attribution 4.0 International License (CC BY 4.0). The original work can be found in reference [197].

alginate hydrogel. These alginate-PCL scaffolds demonstrated a fourfold increase in compressive modulus and better elastic recovery, attributed to PCL's elasticity. Additionally, the nanofibers enhanced fibroblast proliferation by 1.8 times by increasing scaffold porosity.

John et al. [204] developed a technique to make 3D scaffolds with patterned macrochannels. They used 3D printed scaffolds along with poly( $\epsilon$ -caprolactone) (PCL)/gelatin short electrospun nanofibers. The resulting nanofiber aerogels had patterned macrochannels and anisotropic microchannels formed by freeze-casting with 3D-printed sacrificial templates. These scaffolds had single or multiple layers of macrochannels resembling the 3D-printed templates. Aligned microchannels, created through partially anisotropic freezing, acted as interconnected pores between the templated macrochannels. The scaffold's effectiveness was assessed using an osteoblastic cell line (MC3T3-E1). The cells successfully migrated into the templated aerogel scaffold, as shown in Figure 20.

#### 4.6 | Remaining Challenges and Future Directions in the Combination

While merging ES and 3D printing techniques brings innovative capability to ECM scaffold design, it introduces several challenges. The complexity of fusing these two advanced technologies complicates the production process and raises costs. Additionally, poor adhesion between layers may cause delamination, impacting the scaffold's structural integrity. Achieving consistent quality and precise fiber placement during manufacturing demands accurate equipment calibration. Scaling up the production of ECM-mimicking scaffolds for commercial and medical applications poses several challenges because of its detailed, labor-intensive, and time-consuming nature. The ES process, while being effective at creating nanoscale fibers, is inherently slow, and limits its scalability for large-scale production. Integrating ES with 3D printing adds complexity, as it requires precise alignment of nanoscale fibers with macroscale printed structures. Material

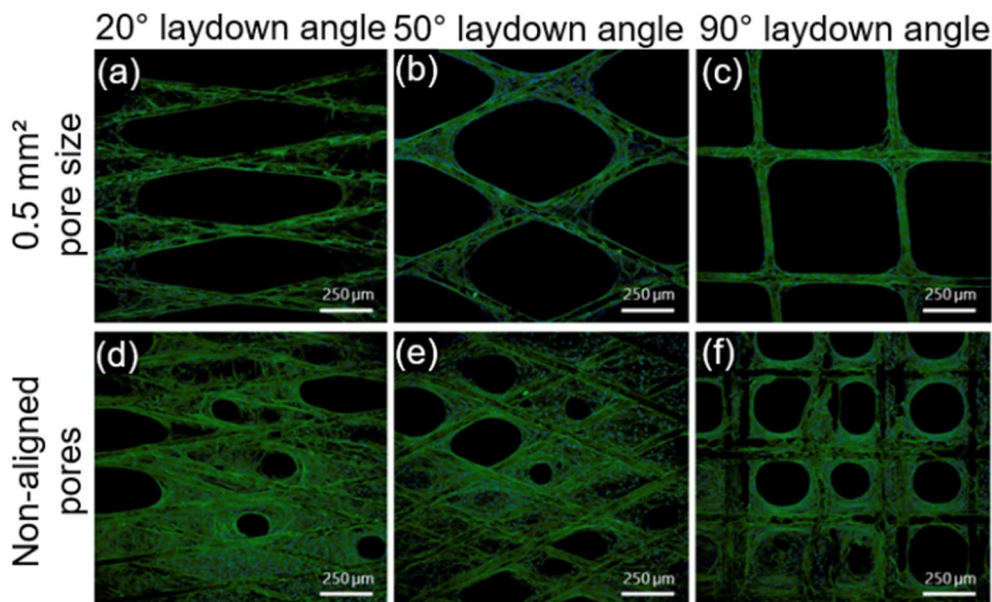


**FIGURE 19** | Fluorescence microscopy images of MC3T3-E1 cells cultured for 3 weeks on PCL scaffolds with fibers in consecutive layers not precisely stacked. The scaffolds were fabricated at laydown angles of 20°, 50°, and 90°, featuring (a–c) aligned pores (0.5 mm<sup>2</sup>) and (d–f) non-aligned pores [199]. Reproduced with permission from Elsevier.

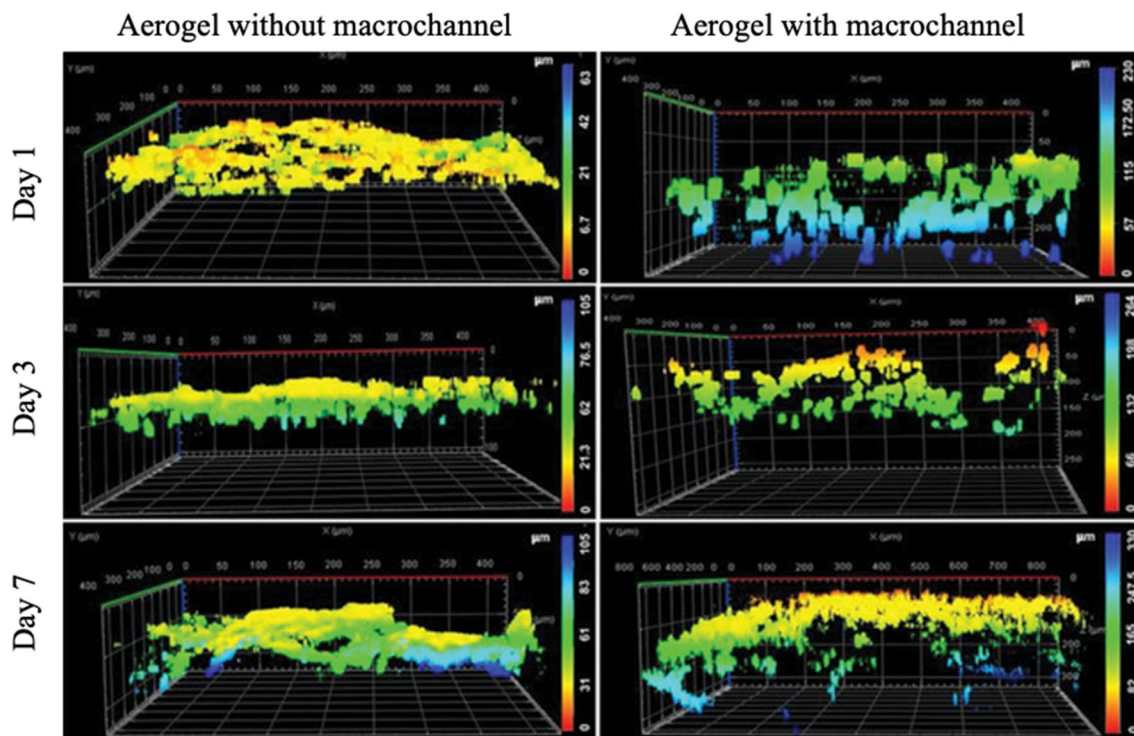


**FIGURE 20** | The MC3T3-E1 cell migration on PCL/gelatin short nanofiber-composed 3D aerogels without and with patterned macrochannels by measuring the depth of the cells on the aerogels in micrometers from the 3D confocal images [204]. Reproduced with permission from John Wiley and Sons.

compatibility further complicates the process, as each technique often relies on different polymers or solvents. Ensuring the production of consistent, high-quality scaffolds at scale while meeting strict medical standards adds another layer of difficulty. For instance, incorporating electrospun nanofibers into bio-inks for 3D printing introduces additional steps like dehydration, freeze-drying, and cross-linking making the process even more time-intensive [205].

To overcome these obstacles and fully exploit the capabilities of these combined technologies for TE, future strategies could focus on developing new materials that enhance layer adhesion to reduce delamination. Future solutions could involve the use of smart materials that are designed to enhance adhesion between electrospun fibers and printed layers. Moreover, specific innovations, such as developing bioinks that support cell viability and promote tissue integration, will be instrumental in enhancing

the functionality of 3D-printed scaffolds. For post-processing, better control of fiber deposition and using solvent-free or bioactive coatings during printing can save time and prevent damaging the structure. Combining functionalization with printing could simplify the process. Incorporating smart materials that can respond to changes in their environment, such as pH, temperature, or specific biochemical signals can provide dynamic capabilities to the scaffolds, facilitating better integration with host tissues. Additionally, exploring sustainable practices, such as using biodegradable or recycled materials in the production of bioinks, will not only reduce costs but also promote environmental responsibility in scaffold fabrication.

Advancements in automation and refined process controls could simplify operations and ensure consistent quality. Automated systems can manage intricate, repetitive steps with high precision, reducing the variability that often occurs with manual handling. Creating standardized protocols and automated systems for sequential fabrication can reduce human error and improve consistency. The advent of modular production systems capable of seamlessly transitioning between ES and 3D printing will streamline the manufacturing process, allowing for efficient scaling from small to large production. Combining 3D printing and ES into one system for hybrid fabrication can simplify the process and lower costs. Using materials that work with both techniques and optimizing the process in real-time can reduce defects. While advancements in artificial intelligence (AI) facilitate process optimization and material design, ensuring consistent quality and performance in scaffold production. These tools can simulate production scenarios, analyze large datasets, and predict outcomes based on varying input conditions, thus enhancing overall process efficiency. Together, these materials and technologies promise to advance the field of TE by enabling the creation of more effective and functional scaffolds.

Innovative equipment designs capable of seamless mode transitions, alongside sophisticated software solutions for process optimization, would further streamline production. In coaxial printing, improving nozzle design and using advanced materials can prevent clogs and increase precision. Making coaxial printing systems more affordable and automated will make the technology more accessible. Future advancements in biofabrication, including faster cross-linking methods and streamlined preparation steps, can help mitigate these issues. Cross-linking techniques enhance the mechanical stability of softer materials such as PEG. In addition, AI-driven systems can enable adaptive manufacturing processes that learn from previous production runs, optimizing parameters in real-time to maintain consistent quality. Therefore, the gap between lab and clinical scalability will narrow as more efficient preparation techniques emerge.

Furthermore, encouraging collaboration across fields such as materials science, engineering, and biotechnology could accelerate the development of effective solutions. Such partnerships allow for the exchange of specialized knowledge in areas like advanced fabrication techniques, biological insights, and precision engineering. This collective expertise helps overcome challenges like optimizing fiber biocompatibility, precisely controlling immune responses, and translating small animal study findings to human use [206]. Clinical translation is limited by insufficient large animal studies, which are crucial for understanding

the immune response in more complex organisms. Addressing these challenges can involve using organs-on-chips, innovative microfluidic devices that simulate human organ structure and function with living cells [207]. These models provide more accurate and ethical disease models, enhancing our understanding of human physiology beyond traditional methods.

By addressing these multifaceted challenges through targeted technological advancements, the combination of ES and 3D printing can significantly improve the design and production of advanced ECM scaffolds.

## 5 | Conclusions

The integration of ES and 3D printing technologies represents a significant advancement in scaffold fabrication, particularly in the fields of TE and regenerative medicine. Each method has its own set of strengths and challenges, but their combination is particularly powerful, producing scaffolds that closely replicate the ECM scaffold to enhance tissue regeneration. There are several approaches to combine those two techniques. The hybrid approach, combining ES and 3D printing, emerges as the best method for scaffold fabrication for several reasons. First, 3D printing allows for precise control over the scaffold's macrostructure, creating complex geometries with pre-determined pore sizes essential for cell migration and nutrient diffusion. On the other hand, ES can deposit nanofibrous layers that mimic the natural fibrous structure of the ECM, providing a high surface area for cell adhesion and proliferation. This dual-scale approach addresses the limitations of each technique alone and ensures a more biomimetic scaffold.

Key variables in this dual process include several parameters to affect electrospun fiber morphology. In 3D printing, layer thickness, orientation, and temperature are critical for attaining the scaffold's macrostructural traits. In addition, effective scaffold creation involves optimizing material selection to ensure both biocompatibility and biodegradability, controlling porosity and pore size to aid tissue integration and vascularization, and enhancing surface features to foster better cellular interactions.

Nevertheless, blending these technologies brings new challenges, including greater complexity, higher costs, and probable issues like delamination, which can affect the structural integrity of the scaffolds. The exact placement of fibers and the labor-intensive manufacturing process make it difficult to scale up production. Looking ahead, the future of using ES and 3D printing for scaffold fabrication is very favorable, with countless improvements on the way. Innovations in bioinks and polymers are expected to boost the functionality and biological effectiveness of the scaffolds. Moreover, Future developments could involve adding multiple ES heads to 3D printers, allowing for the precise placement of different nanofibers in scaffolds. This could enhance scaffold design and support specific cell functions or differentiation, advancing TE and regenerative medicine. Furthermore, better printer designs and software improvements will likely allow for more precise fiber placement and improved scaffold architecture. The growing applications in regenerative medicine, such as creating complex tissue structures and even whole organs, could reform transplant medicine and other medical fields.



## Acknowledgments

Project no. TKP-9-8/PALY-2021 has been implemented with the support provided by the Ministry of Culture and Innovation of Hungary from the National Research, Development, and Innovation Fund, financed under the TKP2021-EGA funding scheme. The research reported in this article was supported by the H2020-MSCA RISE No. 872152—GREEN-MAP project of the European Union. The research reported in this article was supported by the National Research, Development, and Innovation Office (FK 138501). Kolos Molnár is thankful for the support of the János Bolyai Research Scholarship of the Hungarian Academy of Sciences.

## Conflicts of Interest

The authors declare no conflicts of interest.

## References

1. J. F. Bateman, R. P. Boot-Handford, and S. R. Lamandé, “Genetic Diseases of Connective Tissues: Cellular and Extracellular Effects of ECM Mutations,” *Nature Reviews Genetics* 10 (2009): 173–183, <https://doi.org/10.1038/nrg2520>.
2. C. Frantz, K. M. Stewart, and V. M. Weaver, “The Extracellular Matrix at a Glance,” *Journal of Cell Science* 123 (2010): 4195–4200, <https://doi.org/10.1242/jcs.023820>.
3. M. Keshvardoostchokami, S. S. Majidi, P. Huo, R. Ramachandran, M. Chen, and B. Liu, “Electrospun Nanofibers of Natural and Synthetic Polymers as Artificial Extracellular Matrix for Tissue Engineering,” *Nanomaterials* 11 (2020): 21, <https://doi.org/10.3390/nano11010021>.
4. A. Acuna, M. A. Drakopoulos, Y. Leng, C. J. Goergen, and S. Calve, “Three-Dimensional Visualization of Extracellular Matrix Networks During Murine Development,” *Developmental Biology* 435 (2018): 122–129, <https://doi.org/10.1016/j.ydbio.2017.12.022>.
5. M. Saito and K. Marumo, “Effects of Collagen Crosslinking on Bone Material Properties in Health and Disease,” *Calcified Tissue International* 97 (2015): 242–261, <https://doi.org/10.1007/s00223-015-9985-5>.
6. N. K. Karamanos, A. D. Theocharis, Z. Piperigkou, et al., “A Guide to the Composition and Functions of the Extracellular Matrix,” *FEBS Journal* 288 (2021): 6850–6912, <https://doi.org/10.1111/febs.15776>.
7. X. Lin, S. Patil, Y.-G. Gao, and A. Qian, “The Bone Extracellular Matrix in Bone Formation and Regeneration,” *Frontiers in Pharmacology* 11 (2020): 757, <https://doi.org/10.3389/fphar.2020.00757>.
8. L. G. Griffith and G. Naughton, “Tissue Engineering – Current Challenges and Expanding Opportunities,” *Science* 295 (2002): 1009–1014, <https://doi.org/10.1126/science.1069210>.
9. G. G. Walmsley, A. McArdle, R. Tevlin, et al., “Nanotechnology in Bone Tissue Engineering,” *Nanomedicine: Nanotechnology, Biology and Medicine* 11 (2015): 1253–1263, <https://doi.org/10.1016/j.nano.2015.02.013>.
10. R. Langer, J. P. Vacanti, C. A. Vacanti, A. Atala, L. E. Freed, and G. Vunjak-Novakovic, “Tissue Engineering: Biomedical Applications,” *Tissue Engineering* 1 (1995): 151–161, <https://doi.org/10.1089/ten.1995.1.151>.
11. K. F. Ren, M. Hu, H. Zhang, et al., “Layer-By-Layer Assembly as a Robust Method to Construct Extracellular Matrix Mimic Surfaces to Modulate Cell Behavior,” *Progress in Polymer Science* 92 (2019): 1–34, <https://doi.org/10.1016/j.progpolymsci.2019.02.004>.
12. J. K. Carrow and A. K. Gaharwar, “Bioinspired Polymeric Nanocomposites for Regenerative Medicine,” *Macromolecular Chemistry and Physics* 216 (2015): 248–264, <https://doi.org/10.1002/macp.201400427>.
13. A. Keirouz, M. Chung, J. Kwon, G. Fortunato, and N. Radacsi, “2D and 3D Electrospinning Technologies for the Fabrication of Nanofibrous Scaffolds for Skin Tissue Engineering: A Review,” *Wiley Interdisciplinary Reviews. Nanomedicine and Nanobiotechnology* 12 (2020): e1626, <https://doi.org/10.1002/wnan.1626>.
14. E. Zdraveva and B. Mijovic, *Frontier Electrospun Fibers for Nanomedical Applications* (London, United Kingdom: IntechOpen, 2023).
15. G. Belgheisi, M. H. Nazarpak, and M. Solati-Hashjin, “Fabrication and Evaluation of Combined 3D Printed/Pamidronate-Layered Double Hydroxides Enriched Electrospun Scaffolds for Bone Tissue Engineering Applications,” *Applied Clay Science* 225 (2022): 106538, <https://doi.org/10.1016/j.clay.2022.106538>.
16. E. Ewaldz, J. M. Rinehart, M. Miller, and B. Brettmann, “Processability of Thermoelectric Ultrafine Fibers via Electrospinning for Wearable Electronics,” *ACS Omega* 8 (2023): 30239–30246, <https://doi.org/10.1021/acsomega.3c03019>.
17. X. Cao, W. Chen, P. Zhao, Y. Yang, and D.-G. Yu, “Electrospun Porous Nanofibers: Pore-Forming Mechanisms and Applications for Photocatalytic Degradation of Organic Pollutants in Wastewater,” *Polymers* 14 (2022): 3990, <https://doi.org/10.3390/polym14193990>.
18. L. Li, Z. Chen, F. Pan, et al., “Electrospinning Technology on One Dimensional Microwave Absorbers: Fundamentals, Current Progress, and Perspectives,” *Chemical Engineering Journal* 470 (2023): 144236, <https://doi.org/10.1016/j.cej.2023.144236>.
19. J. Lannutti, D. Reneker, T. Ma, D. Tomasko, and D. Farson, “Electrospinning for Tissue Engineering Scaffolds,” *Materials Science and Engineering: C* 27 (2007): 504–509, <https://doi.org/10.1016/j.msec.2006.05.019>.
20. M. Liu, X.-P. Duan, Y.-M. Li, D.-P. Yang, and Y.-Z. Long, “Electrospun Nanofibers for Wound Healing,” *Materials Science and Engineering: C* 76 (2017): 1413–1423, <https://doi.org/10.1016/j.msec.2017.03.034>.
21. H. Kesici Güler and F. Cengiz Callioğlu, “A New Composite Nanofibrous Biomaterial Development for Drug Delivery Applications,” *Express Polymer Letters* 17 (2023): 487–501, <https://doi.org/10.3144/expresspolymlett.2023.36>.
22. Z. Yang, X. Zhang, Z. Qin, et al., “Irflow Synergistic Needleless Electrospinning of Instant Noodle-Like Curly Nanofibrous Membranes for High-Efficiency Air Filtration,” *Small* 18 (2022): 2107250, <https://doi.org/10.1002/sml.202107250>.
23. L. Cao, Y. Si, X. Yin, J. Yu, and B. Ding, “Ultralight and Resilient Electrospun Fiber Sponge With a Lamellar Corrugated Microstructure for Effective Low-Frequency Sound Absorption,” *ACS Applied Materials & Interfaces* 11 (2019): 35333–35342, <https://doi.org/10.1021/acsami.9b12444>.
24. J. Avossa, R. Paolesse, C. Di Natale, et al., “Electrospinning of Polystyrene/Polyhydroxybutyrate Nanofibers Doped With Porphyrin and Graphene for Chemiresistor Gas Sensors,” *Nanomaterials* 9 (2019): 280, <https://doi.org/10.3390/nano9020280>.
25. S. Sriwichai and S. Phanichphant, “Fabrication and Characterization of Electrospun Poly (3-Aminobenzylamine)/Functionalized Multi-Walled Carbon Nanotubes Composite Film for Electrochemical Glucose Biosensor,” *Express Polymer Letters* 16 (2022): 439–450, <https://doi.org/10.3144/expresspolymlett.2022.32>.
26. K. Czarnecka, M. Wojasiński, T. Ciach, and P. Sajkiewicz, “Solution Blow Spinning of Polycaprolactone-Rheological Determination of Spinnability and the Effect of Processing Conditions on Fiber Diameter and Alignment,” *Materials* 14 (2021): 1463, <https://doi.org/10.3390/ma14061463>.
27. B. K. Tarus, N. Fadel, A. Al-Oufy, and M. El-Messiry, “Investigation of Mechanical Properties of Electrospun Poly (Vinyl Chloride) Polymer Nanoengineered Composite,” *Journal of Engineered Fibers and Fabrics* 15 (2020): 1558925020982569, <https://doi.org/10.1177/1558925020982569>.

28. P. Gupta, C. Elkins, T. E. Long, and G. L. Wilkes, "Electrospinning of Linear Homopolymers of Poly (Methyl Methacrylate): Exploring Relationships Between Fiber Formation, Viscosity, Molecular Weight and Concentration in a Good Solvent," *Polymer* 46 (2005): 4799–4810, <https://doi.org/10.1016/j.polymer.2005.04.021>.
29. S. L. Shenoy, W. D. Bates, H. L. Frisch, and G. E. Wnek, "Role of Chain Entanglements on Fiber Formation During Electrospinning of Polymer Solutions: Good Solvent, Non-Specific Polymer–Polymer Interaction Limit," *Polymer* 46 (2005): 3372–3384, <https://doi.org/10.1016/j.polymer.2005.03.011>.
30. C. G. Reyes and J. P. Lagerwall, "Disruption of Electrospinning due to Water Condensation Into the Taylor Cone," *ACS Applied Materials & Interfaces* 12 (2020): 26566–26576, <https://doi.org/10.1021/acsami.0c03338>.
31. B. Pant, M. Park, and S. J. Park, "Drug Delivery Applications of Core-Sheath Nanofibers Prepared by Coaxial Electrospinning: A Review," *Pharmaceutics* 11 (2019): 11, <https://doi.org/10.3390/pharmaceutics11070305>.
32. Z. M. Huang, Y. Z. Zhang, M. Kotaki, and S. Ramakrishna, "A Review on Polymer Nanofibers by Electrospinning and Their Applications in Nanocomposites," *Composites Science and Technology* 63 (2003): 2223–2253, [https://doi.org/10.1016/S0266-3538\(03\)00178-7](https://doi.org/10.1016/S0266-3538(03)00178-7).
33. M. A. A. De Pra, R. M. Ribeiro-do-Valle, M. Maraschin, and B. Veleirinho, "Effect of Collector Design on the Morphological Properties of Polycaprolactone Electrospun Fibers," *Materials Letters* 193 (2017): 154–157, <https://doi.org/10.1016/j.matlet.2017.01.102>.
34. J. Xue, T. Wu, Y. Dai, and Y. Xia, "Electrospinning and Electrospun Nanofibers: Methods, Materials, and Applications," *Chemical Reviews* 119 (2019): 5298–5415, <https://doi.org/10.1021/acs.chemrev.8b00593>.
35. L. Weng and J. Xie, "Smart Electrospun Nanofibers for Controlled Drug Release: Recent Advances and New Perspectives," *Current Pharmaceutical Design* 21 (2015): 1944–1959, <https://doi.org/10.2174/1381612821666150302151959>.
36. Z. A. Raza, A. R. Naeem, R. Shafi, and S. Abid, "Chitosan-Incorporated Poly (Hydroxybutyrate) Porous Electrospun Scaffold for Potential Biomedical Applications," *Polymer Bulletin* 81 (2024): 1691–1705, <https://doi.org/10.1007/s00289-023-04795-5>.
37. R. CeCe, L. Jining, M. Islam, J. G. Korvink, and B. Sharma, "An Overview of the Electrospinning of Polymeric Nanofibers for Biomedical Applications Related to Drug Delivery," *Advanced Engineering Materials* 26 (2024): 2301297, <https://doi.org/10.1002/adem.202301297>.
38. R. Dimri, S. Mall, S. Sinha, et al., "Role of Microalgae as a Sustainable Alternative of Biopolymers and Its Application in Industries," *Plant Science Today* 10 (2023): 8–18, <https://doi.org/10.14719/pst.2460>.
39. S. A. Sell, M. J. McClure, K. Garg, P. S. Wolfe, and G. L. Bowlin, "Electrospinning of Collagen/Biopolymers for Regenerative Medicine and Cardiovascular Tissue Engineering," *Advanced Drug Delivery Reviews* 61 (2009): 1007–1019, <https://doi.org/10.1016/j.addr.2009.07.012>.
40. S. Pina, J. M. Oliveira, and R. L. Reis, "Natural-Based Nanocomposites for Bone Tissue Engineering and Regenerative Medicine: A Review," *Advanced Materials* 27 (2015): 1143–1169, <https://doi.org/10.1002/adma.201403354>.
41. J.-M. Raquez, Y. Habibi, M. Murariu, and P. Dubois, "Polylactide (PLA)-Based Nanocomposites," *Progress in Polymer Science* 38 (2013): 1504–1542, <https://doi.org/10.1016/j.progpolymsci.2013.05.014>.
42. S. Jacobsen, H. Fritz, P. Degée, P. Dubois, and R. Jérôme, "Polylactide (PLA)—a New Way of Production," *Polymer Engineering & Science* 39 (1999): 1311–1319, <https://doi.org/10.1002/pen.11518>.
43. A. Leonés, A. Mujica-Garcia, M. P. Arrieta, et al., "Organic and Inorganic PCL-Based Electrospun Fibers," *Polymers* 12 (2020): 1325, <https://doi.org/10.3390/polym12061325>.
44. L. N. Luduena, V. A. Alvarez, and A. Vazquez, "Processing and Microstructure of PCL/Clay Nanocomposites," *Materials Science and Engineering A* 460 (2007): 121–129, <https://doi.org/10.1016/j.msea.2007.01.104>.
45. H. Jeong, J. Rho, J.-Y. Shin, D. Y. Lee, T. Hwang, and K. J. Kim, "Mechanical Properties and Cytotoxicity of PLA/PCL Films," *Biomedical Engineering Letters* 8 (2018): 267–272, <https://doi.org/10.1007/s13534-018-0065-4>.
46. F.-J. Li, J.-Z. Liang, S.-D. Zhang, and B. Zhu, "Tensile Properties of Polylactide/Poly (Ethylene Glycol) Blends," *Journal of Polymers and the Environment* 23 (2015): 407–415, <https://doi.org/10.1007/s10924-015-0718-7>.
47. K. Y. Lee, J. Shim, and H. G. Lee, "Mechanical Properties of Gellan and Gelatin Composite Films," *Carbohydrate Polymers* 56 (2004): 251–254, <https://doi.org/10.1016/j.carbpol.2003.04.001>.
48. Y. Rao, "Gelatin–Clay Nanocomposites of Improved Properties," *Polymer* 48 (2007): 5369–5375, <https://doi.org/10.1016/j.polymer.2007.06.068>.
49. M. A. Khan, R. A. Khan, F. G. Noor, M. Rahman, and M. Noor-A-alam, "Studies on the Mechanical Properties of Gelatin and Its Blends With Vinyltrimethoxysilane: Effect of Gamma Radiation," *Polymer-Plastics Technology and Engineering* 48 (2009): 808–813, <https://doi.org/10.1080/03602550902994854>.
50. Q. Wu, E. Jungstedt, M. Šoltéssová, N. E. Mushi, and L. A. Berglund, "High Strength Nanostructured Films Based on Well-Preserved  $\beta$ -Chitin Nanofibrils," *Nanoscale* 11 (2019): 11001–11011, <https://doi.org/10.1039/C9NR02870F>.
51. H. Le, S. Qu, R. Mackay, and R. Rothwell, "Fabrication and Mechanical Properties of Chitosan Composite Membrane Containing Hydroxyapatite Particles," *Journal of Advanced Ceramics* 1 (2012): 66–71, <https://doi.org/10.1007/s40145-012-0007-z>.
52. T. Monia, "Sustainable Natural Biopolymers for Biomedical Applications," *Journal of Thermoplastic Composite Materials* 37 (2024): 2505–2524, <https://doi.org/10.1177/08927057231214468>.
53. S. Bhatia and S. Bhatia, *Natural Polymer Drug Delivery Systems* (Basel, Switzerland: Springer International Publishing, 2016), 95–118, [https://doi.org/10.1007/978-3-319-41129-3\\_3](https://doi.org/10.1007/978-3-319-41129-3_3).
54. N. F. Mazuki, M. A. Saadiah, A. F. Fuzlin, N. M. Khan, and A. S. Samsudin, "Basic Aspects and Properties of Biopolymers," in *Biopolymers in Nutraceuticals and Functional Foods*, eds. S. Gopi, P. Balakrishnan, and M. Bračić (Cambridge, United Kingdom: Royal Society of Chemistry, 2022).
55. M. Milojević, U. Maver, and B. Vihar, "Recent Advances in 3 D Printing in the Design and Application of Biopolymer-Based Scaffolds," *Functional Biomaterials: Design and Development for Biotechnology, Pharmacology, and Biomedicine* 2 (2023): 489–559, <https://doi.org/10.1002/9783527827657.ch17>.
56. M. Jurak, A. E. Wiącek, A. Ładniak, K. Przykaza, and K. Szafran, "What Affects the Biocompatibility of Polymers?," *Advances in Colloid and Interface Science* 294 (2021): 102451, <https://doi.org/10.1016/j.cis.2021.102451>.
57. A. Göpferich, "Mechanisms of Polymer Degradation and Erosion," *Biomaterials* 17 (1996): 103–114, [https://doi.org/10.1016/0142-9612\(96\)85755-3](https://doi.org/10.1016/0142-9612(96)85755-3).
58. M. A. Elsayy, K.-H. Kim, J.-W. Park, and A. Deep, "Hydrolytic Degradation of Polylactic Acid (PLA) and Its Composites," *Renewable and Sustainable Energy Reviews* 79 (2017): 1346–1352, <https://doi.org/10.1016/j.rser.2017.05.143>.
59. M. Rutkowska, K. Krasowska, A. Heimowska, and I. Steinka, "Effect of Modification of Poly ( $\epsilon$ -Caprolactone) on Its Biodegradation in Natural Environments," *International Polymer Science and Technology* 29 (2002): 77–84, <https://doi.org/10.1177/0307174X0202901116>.
60. C. X. F. Lam, D. W. Huttmacher, J.-T. Schantz, M. A. Woodruff, and S. H. Teoh, "Evaluation of Polycaprolactone Scaffold Degradation for 6

- Months In Vitro and In Vivo,” *Journal of Biomedical Materials Research Part A* 90A (2009): 906–919, <https://doi.org/10.1002/jbm.a.32052>.
61. A. Zgoła-Grzeskowiak, T. Grzeskowiak, J. Zembrzuska, and Z. Łukaszewski, “Comparison of Biodegradation of Poly (Ethylene Glycol) S and Poly (Propylene Glycol) S,” *Chemosphere* 64 (2006): 803–809, <https://doi.org/10.1016/j.chemosphere.2005.10.056>.
62. J. Chen, S. K. Spear, J. G. Huddleston, and R. D. Rogers, “Polyethylene Glycol and Solutions of Polyethylene Glycol as Green Reaction Media,” *Green Chemistry* 7 (2005): 64–82, <https://doi.org/10.1039/B413546F>.
63. H. Keles, A. Naylor, F. Clegg, and C. Sammon, “Investigation of Factors Influencing the Hydrolytic Degradation of Single PLGA Microparticles,” *Polymer Degradation and Stability* 119 (2015): 228–241, <https://doi.org/10.1016/j.polymerdegradstab.2015.04.025>.
64. B. S. Zolnik and D. J. Burgess, “Effect of Acidic pH on PLGA Microsphere Degradation and Release,” *Journal of Controlled Release* 122 (2007): 338–344, <https://doi.org/10.1016/j.jconrel.2007.05.034>.
65. Y. Huang, S. Onyeri, M. Siewe, A. Moshfeghian, and S. V. Madihally, “In Vitro Characterization of Chitosan–Gelatin Scaffolds for Tissue Engineering,” *Biomaterials* 26 (2005): 7616–7627, <https://doi.org/10.1016/j.biomaterials.2005.05.036>.
66. F. Sharifi, S. Irani, M. Zandi, M. Soleimani, and S. M. Atyabi, “Comparative of Fibroblast and Osteoblast Cells Adhesion on Surface Modified Nanofibrous Substrates Based on Polycaprolactone,” *Progress in Biomaterials* 5 (2016): 213–222, <https://doi.org/10.1007/s40204-016-0059-1>.
67. Z. A. Alhulaybi, “Fabrication and Characterization of Poly (Lactic Acid)-Based Biopolymer for Surgical Sutures,” *ChemEngineering* 7 (2023): 98, <https://doi.org/10.3390/chemengineering7050098>.
68. J. A. Burdick and K. S. Anseth, “Photoencapsulation of Osteoblasts in Injectable RGD-Modified PEG Hydrogels for Bone Tissue Engineering,” *Biomaterials* 23 (2002): 4315–4323, [https://doi.org/10.1016/S0142-9612\(02\)00176-X](https://doi.org/10.1016/S0142-9612(02)00176-X).
69. H. J. Kim, M. A. Han, J. Y. Shin, et al., “Intra-Articular Delivery of Synovium-Resident Mesenchymal Stem Cells via BMP-7-Loaded Fibrous PLGA Scaffolds for Cartilage Repair,” *Journal of Controlled Release* 302 (2019): 169–180, <https://doi.org/10.1016/j.jconrel.2019.04.002>.
70. A. Oryan and S. Sahviah, “Effectiveness of Chitosan Scaffold in Skin, Bone and Cartilage Healing,” *International Journal of Biological Macromolecules* 104 (2017): 1003–1011, <https://doi.org/10.1016/j.ijbmac.2017.06.124>.
71. A. B. Bello, D. Kim, D. Kim, H. Park, and S.-H. Lee, “Engineering and Functionalization of Gelatin Biomaterials: From Cell Culture to Medical Applications,” *Tissue Engineering Part B: Reviews* 26 (2020): 164–180, <https://doi.org/10.1089/ten.teb.2019.0256>.
72. N. K. Kalita, M. K. Nagar, C. Mudenu, A. Kalamdhad, and V. Katiyar, “Biodegradation of Modified Poly (Lactic Acid) Based Biocomposite Films Under Thermophilic Composting Conditions,” *Polymer Testing* 76 (2019): 522–536, <https://doi.org/10.1016/j.polymeresting.2019.02.021>.
73. J. M. Anderson and M. S. Shive, “Biodegradation and Biocompatibility of PLA and PLGA Microspheres,” *Advanced Drug Delivery Reviews* 28 (1997): 5–24, [https://doi.org/10.1016/S0169-409X\(97\)00048-3](https://doi.org/10.1016/S0169-409X(97)00048-3).
74. D. Da Silva, M. Kaduri, M. Poley, et al., “Biocompatibility, Biodegradation and Excretion of Polylactic Acid (PLA) in Medical Implants and Theranostic Systems,” *Chemical Engineering Journal* 340 (2018): 9–14, <https://doi.org/10.1016/j.cej.2018.01.010>.
75. S. Gautam, A. K. Dinda, and N. C. Mishra, “Fabrication and Characterization of PCL/Gelatin Composite Nanofibrous Scaffold for Tissue Engineering Applications by Electrospinning Method,” *Materials Science and Engineering: C* 33 (2013): 1228–1235, <https://doi.org/10.1016/j.msec.2012.12.015>.
76. T. G. Park, “Degradation of Poly (D, L-Lactic Acid) Microspheres: Effect of Molecular Weight,” *Journal of Controlled Release* 30 (1994): 161–173, [https://doi.org/10.1016/0168-3659\(94\)90263-1](https://doi.org/10.1016/0168-3659(94)90263-1).
77. V. J. Chen and P. X. Ma, “The Effect of Surface Area on the Degradation Rate of Nano-Fibrous Poly (L-Lactic Acid) Foams,” *Biomaterials* 27 (2006): 3708–3715, <https://doi.org/10.1016/j.biomaterials.2006.02.020>.
78. S. Hurrell and R. E. Cameron, “The Effect of Initial Polymer Morphology on the Degradation and Drug Release From Polyglycolide,” *Biomaterials* 23 (2002): 2401–2409, [https://doi.org/10.1016/S0142-9612\(01\)00376-3](https://doi.org/10.1016/S0142-9612(01)00376-3).
79. T. G. Park, “Degradation of Poly (Lactic-Co-Glycolic Acid) Microspheres: Effect of Copolymer Composition,” *Biomaterials* 16 (1995): 1123–1130, [https://doi.org/10.1016/0142-9612\(95\)93575-X](https://doi.org/10.1016/0142-9612(95)93575-X).
80. M. M. Stevens and J. H. George, “Exploring and Engineering the Cell Surface Interface,” *Science* 310 (2005): 1135–1138, <https://doi.org/10.1126/science.1106587>.
81. J. X. Ding, J. Zhang, J. N. Li, et al., “Electrospun Polymer Biomaterials,” *Progress in Polymer Science* 90 (2019): 1–34, <https://doi.org/10.1016/j.progpolymsci.2019.01.002>.
82. M. J. McClure, S. A. Sell, D. G. Simpson, B. H. Walpoth, and G. L. Bowlin, “A Three-Layered Electrospun Matrix to Mimic Native Arterial Architecture Using Polycaprolactone, Elastin, and Collagen: A Preliminary Study,” *Acta Biomaterialia* 6 (2010): 2422–2433, <https://doi.org/10.1016/j.actbio.2009.12.029>.
83. Y. Si, J. Yu, X. Tang, J. Ge, and B. Ding, “Ultralight Nanofibre-Assembled Cellular Aerogels With Superelasticity and Multifunctionality,” *Nature Communications* 5 (2014): 5802, <https://doi.org/10.1038/ncomms6802>.
84. C. Kriegel, K. Kit, D. J. McClements, and J. Weiss, “Electrospinning of Chitosan–Poly (Ethylene Oxide) Blend Nanofibers in the Presence of Micellar Surfactant Solutions,” *Polymer* 50 (2009): 189–200, <https://doi.org/10.1016/j.polymer.2008.09.041>.
85. J. S. C. Lo, W. Daoud, C. Y. Tso, et al., “Optimization of Polylactic Acid-Based Medical Textiles via Electrospinning for Healthcare Apparel and Personal Protective Equipment,” *Sustainable Chemistry and Pharmacy* 30 (2022): 100891, <https://doi.org/10.1016/j.scp.2022.100891>.
86. J. Dai, M. Bai, C. Li, H. Cui, and L. Lin, “The Improvement of Sodium Dodecyl Sulfate on the Electrospinning of Gelatin O/W Emulsions for Production of Core-Shell Nanofibers,” *Food Hydrocolloids* 145 (2023): 109092, <https://doi.org/10.1016/j.foodhyd.2023.109092>.
87. V. Beachley and X. Wen, “Effect of Electrospinning Parameters on the Nanofiber Diameter and Length,” *Materials Science and Engineering: C* 29 (2009): 663–668, <https://doi.org/10.1016/j.msec.2008.10.037>.
88. L. Zhao, C. He, Y. Gao, L. Cen, L. Cui, and Y. Cao, “Preparation and Cytocompatibility of PLGA Scaffolds With Controllable Fiber Morphology and Diameter Using Electrospinning Method,” *Journal of Biomedical Materials Research Part B: Applied Biomaterials* 87 (2008): 26–34, <https://doi.org/10.1002/jbm.b.31060>.
89. T. Eren Boncu and N. Ozdemir, “Electrospinning of Ampicillin Trihydrate Loaded Electrospun PLA Nanofibers I: Effect of Polymer Concentration and PCL Addition on Its Morphology, Drug Delivery and Mechanical Properties,” *International Journal of Polymeric Materials and Polymeric Biomaterials* 71 (2022): 669–676, <https://doi.org/10.1080/00914037.2021.1876057>.
90. X. Geng, O.-H. Kwon, and J. Jang, “Electrospinning of Chitosan Dissolved in Concentrated Acetic Acid Solution,” *Biomaterials* 26 (2005): 5427–5432, <https://doi.org/10.1016/j.biomaterials.2005.01.066>.
91. H. Palak, E. Güler, M. Nofar, and B. Karagüzel Kayaoğlu, “Effects of D-Lactide Content and Molecular Weight on the Morphological, Thermal, and Mechanical Properties of Electrospun Nanofiber Polylactide Mats,” *Journal of Industrial Textiles* 51 (2022): 3030S–3056S, <https://doi.org/10.1177/15280837221090260>.
92. K. Koenig, N. Balakrishnan, S. Hermanns, F. Langensiepen, and G. Seide, “Biobased Dyes as Conductive Additives to Reduce the Diameter



- of Polylactic Acid Fibers During Melt Electrospinning,” *Materials* 13 (2020): 1055, <https://doi.org/10.3390/ma13051055>.
93. D. Sharma and B. K. Satapathy, “Tuning Structural-Response of PLA/PCL Based Electrospun Nanofibrous Mats: Role of Dielectric-Constant and Electrical-Conductivity of the Solvent-System,” *Journal of Biomaterials Science, Polymer Edition* 33 (2022): 1759–1793, <https://doi.org/10.1080/09205063.2022.2073427>.
94. M. K. Abdulkadhim and S. A. Habeeb, “The Possibility of Producing Uniform Nanofibers From Blends of Natural Biopolymers,” *Materials Performance and Characterization* 11 (2022): 313–323, <https://doi.org/10.1520/MPC20220045>.
95. Z. Liu, S. Ramakrishna, I. Ahmed, C. Rudd, and X. Liu, “Rheological, Surface Tension and Conductivity Insights on the Electrospinnability of Poly (Lactic-Co-Glycolic Acid)-Hyaluronic Acid Solutions and Their Correlations With the Nanofiber Morphological Characteristics,” *Polymers* 14 (2022): 4411, <https://doi.org/10.3390/polym14204411>.
96. J. Sun, S. L. Perry, and J. D. Schiffman, “Electrospinning Nanofibers From Chitosan/Hyaluronic Acid Complex Coacervates,” *Biomacromolecules* 20 (2019): 4191–4198, <https://doi.org/10.1021/acs.biomac.9b01072>.
97. S. Sheikhzadeh, M. Alizadeh Khaledabad, and H. Almasi, “Fabrication of Electrospun Polycaprolactone/Xanthan Nanofibers: Modeling and Optimization of Electrospinning Parameters by Central Composite Design,” *Journal of Polymers and the Environment* 31 (2023): 1536–1552, <https://doi.org/10.1007/s10924-022-02703-y>.
98. L. A. Bosworth and S. Downes, “Acetone, a Sustainable Solvent for Electrospinning Poly ( $\epsilon$ -Caprolactone) Fibres: Effect of Varying Parameters and Solution Concentrations on Fibre Diameter,” *Journal of Polymers and the Environment* 20 (2012): 879–886, <https://doi.org/10.1007/s10924-012-0436-3>.
99. S. S. Abdelhady, A. El-Desouky, A. Kassab, W. Barakat, and S. H. Zoalfakar, “Optimization of Electrospun Chitosan/Polyethylene Oxide Hybrid Nanofibril Composite via Response Surface Methodology,” *Journal of Thermoplastic Composite Materials* 37 (2023): 885–909, <https://doi.org/10.1177/08927057231188017>.
100. W. J. Li, C. T. Laurencin, E. J. Caterson, R. S. Tuan, and F. K. Ko, “Electrospun Nanofibrous Structure: A Novel Scaffold for Tissue Engineering,” *Journal of Biomedical Materials Research* 60 (2002): 613–621, <https://doi.org/10.1002/jbm.10167>.
101. A. A. Dokuchaeva, T. P. Timchenko, E. V. Karpova, S. V. Vladimirov, I. A. Soynov, and I. Y. Zhuravleva, “Effects of Electrospinning Parameter Adjustment on the Mechanical Behavior of Poly- $\epsilon$ -Caprolactone Vascular Scaffolds,” *Polymers* 14 (2022): 349, <https://doi.org/10.3390/polym14020349>.
102. V. Sencadas, D. M. Correia, A. Areias, et al., “Determination of the Parameters Affecting Electrospun Chitosan Fiber Size Distribution and Morphology,” *Carbohydrate Polymers* 87 (2012): 1295–1301, <https://doi.org/10.1016/j.carbpol.2011.09.017>.
103. T. D. Brown, P. D. Dalton, and D. W. Huttmacher, “Direct Writing by Way of Melt Electrospinning,” *Advanced Materials* 23 (2011): 5651–5657, <https://doi.org/10.1002/adma.201103482>.
104. A. Wagner, V. Poursorkhabi, A. K. Mohanty, and M. Misra, “Analysis of Porous Electrospun Fibers From Poly (L-Lactic Acid)/Poly (3-Hydroxybutyrate-Co-3-Hydroxyvalerate) Blends,” *ACS Sustainable Chemistry & Engineering* 2 (2014): 1976–1982, <https://doi.org/10.1021/sc5000495>.
105. D. Han, S. Sherman, S. Filocamo, and A. J. Steckl, “Long-Term Antimicrobial Effect of Nisin Released From Electrospun Triaxial Fiber Membranes,” *Acta Biomaterialia* 53 (2017): 242–249, <https://doi.org/10.1016/j.actbio.2017.02.029>.
106. B. Zhang, X. Yan, H.-W. He, M. Yu, X. Ning, and Y.-Z. Long, “Solvent-Free Electrospinning: Opportunities and Challenges,” *Polymer Chemistry* 8 (2017): 333–352, <https://doi.org/10.1039/c6py01898j>.
107. A. Hudecki, J. Gola, S. Ghavami, et al., “Structure and Properties of Slow-Resorbing Nanofibers Obtained by (Co-Axial) Electrospinning as Tissue Scaffolds in Regenerative Medicine,” *PeerJ* 5 (2017): e4125, <https://doi.org/10.7717/peerj.4125/supp-1>.
108. G. C. Ingavle and J. K. Leach, “Advancements in Electrospinning of Polymeric Nanofibrous Scaffolds for Tissue Engineering,” *Tissue Engineering Part B: Reviews* 20 (2014): 277–293, <https://doi.org/10.1089/ten.teb.2013.0276>.
109. G. Yan, Z. Yang, X. Zhang, et al., “Antibacterial Biodegradable Nanofibrous Membranes by Hybrid Needleless Electrospinning for High-Efficiency Particulate Matter Removal,” *Chemical Engineering Journal* 461 (2023): 142137, <https://doi.org/10.1016/j.cej.2023.142137>.
110. D. Han and P.-I. Gouma, “Electrospun Bioscaffolds That Mimic the Topology of Extracellular Matrix,” *Nanomedicine: Nanotechnology, Biology and Medicine* 2 (2006): 37–41, <https://doi.org/10.1016/j.nano.2006.01.002>.
111. W. Ji, Y. Sun, F. Yang, et al., “Bioactive Electrospun Scaffolds Delivering Growth Factors and Genes for Tissue Engineering Applications,” *Pharmaceutical Research* 28 (2011): 1259–1272, <https://doi.org/10.1007/s11095-010-0320-6>.
112. Y. Mao, Y. Chen, W. Li, et al., “Physiology-Inspired Multilayer Nanofibrous Membranes Modulating Endogenous Stem Cell Recruitment and Osteo-Differentiation for Staged Bone Regeneration,” *Advanced Healthcare Materials* 11 (2022): 2201457, <https://doi.org/10.1002/adhm.202201457>.
113. T. Abudula, U. Saeed, A. Memic, K. Gauthaman, M. A. Hussain, and H. Al-Turaif, “Electrospun Cellulose Nano Fibril Reinforced PLA/PBS Composite Scaffold for Vascular Tissue Engineering,” *Journal of Polymer Research* 26 (2019): 1–15, <https://doi.org/10.1007/s10965-022-03234-9>.
114. J. Wang, J. Lin, L. Chen, L. Deng, and W. Cui, “Endogenous Electric-Field-Coupled Electrospun Short Fiber via Collecting Wound Exudation,” *Advanced Materials* 34 (2022): 2108325, <https://doi.org/10.1002/adma.202108325>.
115. D. D. Zong, X. X. Zhang, X. Yin, et al., “Electrospun Fibrous Sponges: Principle, Fabrication, and Applications,” *Advanced Fiber Materials* 4 (2022): 1434–1462, <https://doi.org/10.1007/s42765-022-00202-2>.
116. Y. Li, J. Wang, D. Qian, et al., “Electrospun Fibrous Sponge via Short Fiber for Mimicking 3D ECM,” *Journal of Nanobiotechnology* 19 (2021): 131, <https://doi.org/10.1186/s12951-021-00878-5>.
117. Y. Chen, M. Shafiq, M. Liu, Y. Morsi, and X. Mo, “Advanced Fabrication for Electrospun Three-Dimensional Nanofiber Aerogels and Scaffolds,” *Bioactive Materials* 5 (2020): 963–979, <https://doi.org/10.1016/j.bioactmat.2020.06.023>.
118. J. Zhang, L. Chen, J. Wang, et al., “Multisite Captured Copper Ions via Phosphorus Dendrons Functionalized Electrospun Short Nanofibrous Sponges for Bone Regeneration,” *Advanced Functional Materials* 33 (2023): 2211237, <https://doi.org/10.1002/adfm.202211237>.
119. H. N. Chia and B. M. Wu, “Recent Advances in 3D Printing of Biomaterials,” *Journal of Biological Engineering* 9 (2015): 1–14, <https://doi.org/10.1186/s13036-015-0001-4>.
120. S. D. Shelare, K. R. Aglawe, and P. B. Khope, “Computer Aided Modeling and Finite Element Analysis of 3-D Printed Drone,” *Materials Today Proceedings* 47 (2021): 3375–3379, <https://doi.org/10.1016/j.matpr.2021.07.162>.
121. M. M. Hanon, R. Marczis, and L. Zsidai, “Influence of the 3D Printing Process Settings on Tensile Strength of PLA and HT-PLA,” *Periodica Polytechnica, Mechanical Engineering* 65 (2021): 38–46, <https://doi.org/10.3311/PPme.13683>.
122. K. Kiss-Nagy, G. Simongáti, and P. Ficzer, “Investigation of 3D Printed Underwater Thruster Propellers Using CFD and Structural Simulations,” *Periodica Polytechnica, Mechanical Engineering* 68 (2024): 70–77, <https://doi.org/10.3311/PPme.23795>.

123. S. H. Jariwala, G. S. Lewis, Z. J. Bushman, J. H. Adair, and H. J. Donahue, "3D Printing of Personalized Artificial Bone Scaffolds," *3D Printing and Additive Manufacturing* 2 (2015): 56–64, <https://doi.org/10.1089/3dp.2015.0001>.
124. D. Ma, R. Gao, M. Li, and J. Qiu, "Mechanical and Medical Imaging Properties of 3D-Printed Materials as Tissue Equivalent Materials," *Journal of Applied Clinical Medical Physics* 23 (2022): e13495, <https://doi.org/10.1002/acm2.13495>.
125. Z.-X. Low, Y. T. Chua, B. M. Ray, D. Mattia, I. S. Metcalfe, and D. A. Patterson, "Perspective on 3D Printing of Separation Membranes and Comparison to Related Unconventional Fabrication Techniques," *Journal of Membrane Science* 523 (2017): 596–613, <https://doi.org/10.1016/j.memsci.2016.10.006>.
126. A. V. Do, B. Khorsand, S. M. Geary, and A. K. Salem, "3D Printing of Scaffolds for Tissue Regeneration Applications," *Advanced Healthcare Materials* 4 (2015): 1742–1762, <https://doi.org/10.1002/adhm.201500168>.
127. A. Anandhapadman, A. Venkateswaran, H. Jayaraman, and N. Veerabadrhan Ghone, "Advances in 3D Printing of Composite Scaffolds for the Repairment of Bone Tissue Associated Defects," *Biotechnology Progress* 38 (2022): e3234, <https://doi.org/10.1002/btpr.3234>.
128. L. Zhang, G. Yang, B. N. Johnson, and X. Jia, "Three-Dimensional (3D) Printed Scaffold and Material Selection for Bone Repair," *Acta Biomaterialia* 84 (2019): 16–33, <https://doi.org/10.1016/j.actbio.2018.11.039>.
129. K. Molnár, "Combination of Nanofibers With 3D-Printed or 4D-Printed Structures," *Express Polymer Letters* 18 (2024): 243–244, <https://doi.org/10.3144/expresspolymlett.2024.17>.
130. I. Zein, D. W. Huttmacher, K. C. Tan, and S. H. Teoh, "Fused Deposition Modeling of Novel Scaffold Architectures for Tissue Engineering Applications," *Biomaterials* 23 (2002): 1169–1185, [https://doi.org/10.1016/S0142-9612\(01\)00232-0](https://doi.org/10.1016/S0142-9612(01)00232-0).
131. Z. Weng, J. Wang, T. Senthil, and L. Wu, "Mechanical and Thermal Properties of ABS/Montmorillonite Nanocomposites for Fused Deposition Modeling 3D Printing," *Materials and Design* 102 (2016): 276–283, <https://doi.org/10.1016/j.matdes.2016.04.045>.
132. S. Naghieh, E. Foroozmehr, M. Badrossamay, and M. Kharaziha, "Mechanical and Thermal Properties of ABS/Montmorillonite Nanocomposites for Fused Deposition Modeling 3D Printing," *Materials and Design* 133 (2017): 128–135, <https://doi.org/10.1016/j.matdes.2017.07.051>.
133. T. Qin, X. Li, H. Long, S. Bin, and Y. Xu, "Bioactive Tetracalcium Phosphate Scaffolds Fabricated by Selective Laser Sintering for Bone Regeneration Applications," *Materials* 13 (2020): 2268, <https://doi.org/10.3390/ma13102268>.
134. B. Thavornyutikarn, N. Chantarapanich, K. Sittthiseripratip, G. Thouas, and Q. Chen, "Bone Tissue Engineering Scaffolding: Computer-Aided Scaffolding Techniques," *Progress in Biomaterials* 3 (2014): 61–102, <https://doi.org/10.1007/s40204-014-0026-7>.
135. K. Da Silva, P. Kumar, Y. E. Choonara, L. C. du Toit, and V. Pillay, "Three-Dimensional Printing of Extracellular Matrix (ECM)-Mimicking Scaffolds: A Critical Review of the Current ECM Materials," *Journal of Biomedical Materials Research Part A* 108 (2020): 2324–2350, <https://doi.org/10.1002/jbm.a.36981>.
136. D. Xue, J. Zhang, Y. Wang, D. Mei, and A. C. S. Biomater, "Digital Light Processing-Based 3D Printing of Cell-Seeding Hydrogel Scaffolds With Regionally Varied Stiffness," *ACS Biomaterials Science & Engineering* 5 (2019): 4825–4833, <https://doi.org/10.1021/acsbomaterials.9b00696>.
137. G. Camci-Unal, P. Zorlutuna, and A. Khademhosseini, "Fabrication of Microscale Hydrogels for Tissue Engineering Applications," in *Biofabrication* (Amsterdam, Netherlands: Elsevier, 2013), 59–80.
138. M. B. Kumar, P. Sathiya, and M. Varatharajulu, *Selective Laser Sintering, Advances in Additive Manufacturing Processes* (Singapore: Bentham Science Publishers Pte. Ltd., 2021), 28–47.
139. G. Ratheesh, C. Vaquette, and Y. Xiao, "Patient-Specific Bone Particles Bioprinting for Bone Tissue Engineering," *Advanced Healthcare Materials* 9 (2020): 2001323, <https://doi.org/10.1002/adhm.202001323>.
140. M. T. Poldervaart, B. Goversen, M. De Ruijter, et al., "3D Bioprinting of Methacrylated Hyaluronic Acid (MeHA) Hydrogel With Intrinsic Osteogenicity," *PLoS One* 12 (2017): e0177628, <https://doi.org/10.1371/journal.pone.0177628>.
141. H. Suo, D. Zhang, J. Yin, J. Qian, Z. L. Wu, and J. Fu, "Interpenetrating Polymer Network Hydrogels Composed of Chitosan and Photocrosslinkable Gelatin With Enhanced Mechanical Properties for Tissue Engineering," *Materials Science and Engineering: C* 92 (2018): 612–620, <https://doi.org/10.1016/j.msec.2018.07.016>.
142. M. Fenelon, M. Etchebarne, R. Siadous, et al., "Assessment of Fresh and Preserved Amniotic Membrane for Guided Bone Regeneration in Mice," *Journal of Biomedical Materials Research Part A* 108 (2020): 2044–2056, <https://doi.org/10.1002/jbm.a.36964>.
143. N. A. Chartrain, K. H. Gilchrist, V. B. Ho, and G. J. Klarmann, "3D Bioprinting for the Repair of Articular Cartilage and Osteochondral Tissue," *Bioprinting* 28 (2022): e00239, <https://doi.org/10.1016/j.bprint.2022.e00239>.
144. S. Chae and D.-W. Cho, "Three-Dimensional Bioprinting With Decellularized Extracellular Matrix-Based Bioinks in Translational Regenerative Medicine," *MRS Bulletin* 47 (2022): 70–79, <https://doi.org/10.1557/s43577-021-00260-8>.
145. C. Vyas, *Development of a Multi-Material and Multi-Scale 3d Bioprinted Scaffold for Osteochondral Tissue Engineering* (UK: University of Manchester, 2020).
146. S. M. Hull, L. G. Brunel, and S. C. Heilshorn, "3D Bioprinting of Cell-Laden Hydrogels for Improved Biological Functionality," *Advanced Materials* 34 (2022): 2103691, <https://doi.org/10.1002/adma.202103691>.
147. W. Park, G. Gao, and D.-W. Cho, "Tissue-Specific Decellularized Extracellular Matrix Bioinks for Musculoskeletal Tissue Regeneration and Modeling Using 3D Bioprinting Technology," *International Journal of Molecular Sciences* 22 (2021): 7837, <https://doi.org/10.3390/ijms22157837>.
148. A. Aazmi, D. Zhang, C. Mazzaglia, et al., "Biofabrication Methods for Reconstructing Extracellular Matrix Mimetics," *Bioactive Materials* 31 (2024): 475–496, <https://doi.org/10.1016/j.bioactmat.2023.08.018>.
149. Z. Wang, L. Wang, T. Li, et al., "3D Bioprinting in Cardiac Tissue Engineering," *Theranostics* 11 (2021): 7948, <https://doi.org/10.7150/thno.61621>.
150. A. Samadi, A. Moammeri, M. Pourmadadi, et al., "Cell Encapsulation and 3D Bioprinting for Therapeutic Cell Transplantation," *ACS Biomaterials Science & Engineering* 9 (2023): 1862–1890, <https://doi.org/10.1021/acsbomaterials.2c01183>.
151. M. Grimaudo, G. Krishnakumar, E. Giusto, et al., "Bioactive Injectable Hydrogels for on Demand Molecule/Cell Delivery and for Tissue Regeneration in the Central Nervous System," *Acta Biomaterialia* 140 (2022): 88–101, <https://doi.org/10.1016/j.actbio.2021.11.038>.
152. A. J. Vernengo, S. Grad, D. Eglin, M. Alini, and Z. Li, "Bioprinting Tissue Analogues With Decellularized Extracellular Matrix Bioink for Regeneration and Tissue Models of Cartilage and Intervertebral Discs," *Advanced Functional Materials* 30 (2020): 1909044, <https://doi.org/10.1002/adfm.201909044>.
153. D. B. Kolesky, K. A. Homan, M. A. Skylar-Scott, and J. A. Lewis, "Three-Dimensional Bioprinting of Thick Vascularized Tissues," *Proceedings of the National Academy of Sciences* 113 (2016): 3179–3184, <https://doi.org/10.1073/pnas.1521342113>.

154. G. S. Hussey, J. L. Dziki, and S. F. Badylak, "Extracellular Matrix-Based Materials for Regenerative Medicine," *Nature Reviews Materials* 3 (2018): 159–173, <https://doi.org/10.1038/s41578-018-0023-x>.
155. C. Li and W. Cui, "3D Bioprinting of Cell-Laden Constructs for Regenerative Medicine," *Engineered Regeneration* 2 (2021): 195–205, <https://doi.org/10.1016/j.engreg.2021.11.005>.
156. J. Huang, J. Xiong, D. Wang, et al., "3D Bioprinting of Hydrogels for Cartilage Tissue Engineering," *Gels* 7 (2021): 144, <https://doi.org/10.3390/gels7030144>.
157. J. H. Shin and H.-W. Kang, "The Development of Gelatin-Based Bio-Ink for Use in 3D Hybrid Bioprinting," *International Journal of Precision Engineering and Manufacturing* 19 (2018): 767–771, <https://doi.org/10.1007/s12541-018-0092-1>.
158. X. Zhang, Y. Liu, Q. Zuo, et al., "3D Bioprinting of Biomimetic Bilayered Scaffold Consisting of Decellularized Extracellular Matrix and Silk Fibroin for Osteochondral Repair," *International Journal of Bioprinting* 7 (2021): 85–98, <https://doi.org/10.18063/ijb.v7i4.401>.
159. W. Lin, M. Chen, T. Qu, J. Li, and Y. Man, "Three-Dimensional Electrospun Nanofibrous Scaffolds for Bone Tissue Engineering," *Journal of Biomedical Materials Research Part B: Applied Biomaterials* 108 (2020): 1311–1321, <https://doi.org/10.1002/jbm.b.34479>.
160. C. P. Barnes, S. A. Sell, E. D. Boland, D. G. Simpson, and G. L. Bowlin, "Nanofiber Technology: Designing the Next Generation of Tissue Engineering Scaffolds," *Advanced Drug Delivery Reviews* 59 (2007): 1413–1433, <https://doi.org/10.1016/j.addr.2007.04.022>.
161. Y. A. Amnieh, S. Ghadirian, N. Mohammadi, M. Shadkhist, and S. Karbasi, "Evaluation of the Effects of Chitosan Nanoparticles on Polyhydroxy Butyrate Electrospun Scaffolds for Cartilage Tissue Engineering Applications," *International Journal of Biological Macromolecules* 249 (2023): 126064, <https://doi.org/10.1016/j.ijbiomac.2023.126064>.
162. B. A. Nerger, P.-T. Brun, and C. M. Nelson, "Marangoni Flows Drive the Alignment of Fibrillar Cell-Laden Hydrogels," *Science Advances* 6 (2020): eaaz7748, <https://doi.org/10.1126/sciadv.aaz7748>.
163. N. Akbari, S. Khorshidi, and A. Karkhaneh, "Effect of Piezoelectricity of Nanocomposite Electrospun Scaffold on Cell Behavior in Bone Tissue Engineering," *Iranian Polymer Journal* 31 (2022): 919–930, <https://doi.org/10.1007/s13726-022-01047-7>.
164. C. M. Murphy and F. J. O'Brien, "Understanding the Effect of Mean Pore Size on Cell Activity in Collagen-Glycosaminoglycan Scaffolds," *Cell Adhesion & Migration* 4 (2010): 377–381, <https://doi.org/10.4161/cam.4.3.11747>.
165. G. Kim, J. Son, S. Park, and W. Kim, "Hybrid Process for Fabricating 3D Hierarchical Scaffolds Combining Rapid Prototyping and Electrospinning," *Macromolecular Rapid Communications* 29 (2008): 1577–1581, <https://doi.org/10.1002/marc.200800277>.
166. G. L. Koons, M. Diba, and A. G. Mikos, "Materials Design for Bone-Tissue Engineering," *Nature Reviews Materials* 5 (2020): 584–603, <https://doi.org/10.1038/s41578-020-0204-2>.
167. R. Sanz-Horta, C. Elvira, A. Gallardo, H. Reinecke, and J. Rodríguez-Hernández, "Fabrication of 3D-Printed Biodegradable Porous Scaffolds Combining Multi-Material Fused Deposition Modeling and Supercritical CO<sub>2</sub> Techniques," *Nanomaterials* 10 (2020): 1080, <https://doi.org/10.3390/nano10061080>.
168. S.-y. Zhang, M. Zhang, X.-y. Li, et al., "Development of a Novel Bioartificial Cornea Using 3D Bioprinting Based on Electrospun Micro-Nanofibrous Decellularized Extracellular Matrix," *Biofabrication* 16 (2024): 025039, <https://doi.org/10.1088/1758-5090/ad35ea>.
169. M. Rahmati, D. K. Mills, A. M. Urbanska, et al., "Electrospinning for Tissue Engineering Applications," *Progress in Materials Science* 117 (2021): 100721, <https://doi.org/10.1016/j.pmatsci.2020.100721>.
170. M. Zhang, S. Xu, R. Wang, et al., "Electrospun Nanofiber/Hydrogel Composite Materials and Their Tissue Engineering Applications," *Journal of Materials Science and Technology* 162 (2023): 157–178, <https://doi.org/10.1016/j.jmst.2023.04.015>.
171. O. A. González Rodríguez, N. C. Ramírez Guerrero, R. G. Casañas Pimentel, M. R. Jaime Fonseca, and E. San Martín Martínez, "Polycaprolactone, Polylactic Acid, and Nanohydroxyapatite Scaffolds Obtained by Electrospinning and 3D Printing for Tissue Engineering," *International Journal of Polymeric Materials and Polymeric Biomaterials* 73 (2024): 1279–1290, <https://doi.org/10.1080/00914037.2023.2277222>.
172. K. Liu, L. Li, J. Chen, et al., "Bone ECM-Like 3D Printing Scaffold With Liquid Crystalline and Viscoelastic Microenvironment for Bone Regeneration," *ACS Nano* 16 (2022): 21020–21035, <https://doi.org/10.1021/acsnano.2c08699>.
173. S.-H. Shin, O. Purevdorj, O. Castano, J. A. Planell, and H.-W. Kim, "A Short Review: Recent Advances in Electrospinning for Bone Tissue Regeneration," *Journal of Tissue Engineering* 3 (2012): 2041731412443530, <https://doi.org/10.1177/2041731412443530>.
174. J. Venugopal, S. Low, A. T. Choon, and S. Ramakrishna, "Interaction of Cells and Nanofiber Scaffolds in Tissue Engineering," *Journal of Biomedical Materials Research Part B: Applied Biomaterials* 84 (2008): 34–48, <https://doi.org/10.1002/jbm.b.30841>.
175. M. Yeo and G. Kim, "Nano/Microscale Topographically Designed Alginate/PCL Scaffolds for Inducing Myoblast Alignment and Myogenic Differentiation," *Carbohydrate Polymers* 223 (2019): 115041, <https://doi.org/10.1016/j.carbpol.2019.115041>.
176. A. Gonzalez-Pujana, T. Carranza, E. Santos-Vizcaino, et al., "Hybrid 3D Printed and Electrospun Multi-Scale Hierarchical Polycaprolactone Scaffolds to Induce Bone Differentiation," *Pharmaceutics* 14 (2022): 2843, <https://doi.org/10.3390/pharmaceutics14122843>.
177. A. Moetazedian, A. Gleadall, X. Han, A. Ekinici, E. Mele, and V. V. Silberschmidt, "Mechanical Performance of 3D Printed Polylactide During Degradation," *Additive Manufacturing* 38 (2021): 101764, <https://doi.org/10.1016/j.addma.2020.101764>.
178. Z. Yang, Z. Song, X. Nie, K. Guo, and Y. Gu, "A Smart Scaffold Composed of Three-Dimensional Printing and Electrospinning Techniques and Its Application in Rat Abdominal Wall Defects," *Stem Cell Research & Therapy* 11 (2020): 1–11, <https://doi.org/10.1186/s13287-020-02042-6>.
179. K. Raje, K. Ohashi, and S. Fujita, "Three-Dimensional Printer-Assisted Electrospinning for Fabricating Intricate Biological Tissue Mimics," *Nanomaterials* 13 (2023): 2913, <https://doi.org/10.3390/nano13222913>.
180. A. B. Touré, E. Mele, and J. K. Christie, "Multi-Layer Scaffolds of Poly(Caprolactone), poly(Glycerol Sebacate) and Bioactive Glasses Manufactured by Combined 3D Printing and Electrospinning," *Nanomaterials* 10 (2020): 626, <https://doi.org/10.3390/nano10040626>.
181. X. Liu, M. Chen, J. Luo, et al., "Immunopolarization-Regulated 3D Printed-Electrospun Fibrous Scaffolds for Bone Regeneration," *Biomaterials* 276 (2021): 121037, <https://doi.org/10.1016/j.biomaterials.2021.121037>.
182. H. He and K. Molnár, "Fabrication of 3D Printed Nanocomposites With Electrospun Nanofiber Interleaves," *Additive Manufacturing* 46 (2021): 102030, <https://doi.org/10.1016/j.addma.2021.102030>.
183. Y. Cao, L. Sun, Z. Liu, et al., "3D Printed-Electrospun PCL/Hydroxyapatite/MWCNTs Scaffolds for the Repair of Subchondral Bone," *Regenerative Biomaterials* 10 (2023): rbac104, <https://doi.org/10.1093/rb/rbac104>.
184. G. Belgheisi, M. H. Nazarpak, and M. Solati-Hashjin, "Microstructure, Mechanical, and In Vitro Performance of a Novel Combination of Layered Double Hydroxides and Polycaprolactone Electrospun/3D Printed Scaffolds for Bone Tissue Engineering," *Fibers and Polymers* 24 (2023): 3085–3099, <https://doi.org/10.1007/s12221-023-00310-9>.



185. N. Z. Laird, T. M. Acri, J. L. Chakka, et al., "Applications of Nanotechnology in 3D Printed Tissue Engineering Scaffolds," *European Journal of Pharmaceutics and Biopharmaceutics* 161 (2021): 15–28, <https://doi.org/10.1016/j.ejpb.2021.01.018>.
186. L. Roseti, V. Parisi, M. Petretta, et al., "Scaffolds for Bone Tissue Engineering: State of the Art and New Perspectives," *Materials Science and Engineering: C* 78 (2017): 1246–1262, <https://doi.org/10.1016/j.msec.2017.05.017>.
187. H. Saniei and S. Mousavi, "Surface Modification of PLA 3D-Printed Implants by Electrospinning With Enhanced Bioactivity and Cell Affinity," *Polymer* 196 (2020): 122467, <https://doi.org/10.1016/j.polymer.2020.122467>.
188. Y. Mao, T. Hoffman, A. Wu, R. Goyal, and J. Kohn, "Cell Type-Specific Extracellular Matrix Guided the Differentiation of Human Mesenchymal Stem Cells in 3D Polymeric Scaffolds," *Journal of Materials Science: Materials in Medicine* 28 (2017): 1–8, <https://doi.org/10.1007/s10856-017-5912-9>.
189. S. Liu, Y. Zheng, R. Liu, and C. Tian, "Preparation and Characterization of a Novel Polylactic Acid/Hydroxyapatite Composite Scaffold With Biomimetic Micro-Nanofibrous Porous Structure," *Journal of Materials Science: Materials in Medicine* 31 (2020): 1–11, <https://doi.org/10.1007/s10856-020-06415-4>.
190. G. Turnbull, J. Clarke, F. Picard, et al., "3D Bioactive Composite Scaffolds for Bone Tissue Engineering," *Bioactive Materials* 3 (2018): 278–314, <https://doi.org/10.1016/j.bioactmat.2017.10.001>.
191. X. Cao and D. Chen, "BMP Signaling and In Vivo Bone Formation," *Gene* 357 (2005): 1–8, <https://doi.org/10.1016/j.gene.2005.06.017>.
192. S. L. Bellis, "Advantages of RGD Peptides for Directing Cell Association With Biomaterials," *Biomaterials* 32 (2011): 4205–4210, <https://doi.org/10.1016/j.biomaterials.2011.02.029>.
193. I. Rajzer, A. Kurowska, A. Jabłoński, et al., "Layered Gelatin/ PLLA Scaffolds Fabricated by Electrospinning and 3D Printing-For Nasal Cartilages and Subchondral Bone Reconstruction," *Materials and Design* 155 (2018): 297–306, <https://doi.org/10.1016/j.matdes.2018.06.012>.
194. R. Rosales-Ibáñez, A. E. Viera-Ruiz, J. V. Cauich-Rodríguez, et al., "Electrospun/3D-Printed PCL Bioactive Scaffold for Bone Regeneration," *Polymer Bulletin* 80 (2023): 2533–2552, <https://doi.org/10.1007/s00289-022-04149-7>.
195. P. S. Zieliński, P. K. R. Gudeti, T. Rikmanspoel, and M. K. Włodarczyk-Biegun, "3D Printing of Bio-Instructive Materials: Toward Directing the Cell," *Bioactive Materials* 19 (2023): 292–327, <https://doi.org/10.1016/j.bioactmat.2022.04.008>.
196. B. Huang, E. Aslan, Z. Jiang, et al., "Engineered Dual-Scale Poly ( $\epsilon$ -Caprolactone) Scaffolds Using 3D Printing and Rotational Electrospinning for Bone Tissue Regeneration," *Additive Manufacturing* 36 (2020): 101452, <https://doi.org/10.1016/j.addma.2020.101452>.
197. C. Vyas, G. Ates, E. Aslan, J. Hart, B. Huang, and P. Bartolo, "Three-Dimensional Printing and Electrospinning Dual-Scale Polycaprolactone Scaffolds With Low-Density and Oriented Fibers to Promote Cell Alignment," *3D Printing and Additive Manufacturing* 7 (2020): 105–113, <https://doi.org/10.1089/3dp.2019.0091>.
198. E. L. Gill, S. Willis, M. Gerigk, et al., "Fabrication of Designable and Suspended Microfibers via Low-Voltage 3D Micropatterning," *ACS Applied Materials & Interfaces* 11 (2019): 19679–19690, <https://doi.org/10.1021/acsami.9b01258>.
199. N. C. Paxton, M. Lanaro, A. Bo, et al., "Design Tools for Patient Specific and Highly Controlled Melt Electrowritten Scaffolds," *Journal of the Mechanical Behavior of Biomedical Materials* 105 (2020): 103695, <https://doi.org/10.1016/j.jmbbm.2020.103695>.
200. Q. Fu, C. Duan, Z. Yan, et al., "Nanofiber-Based Hydrogels: Controllable Synthesis and Multifunctional Applications," *Macromolecular Rapid Communications* 39 (2018): 1800058, <https://doi.org/10.1002/marc.201800058>.
201. Y. Yu, S. Hua, M. Yang, et al., "Fabrication and Characterization of Electrospinning/3D Printing Bone Tissue Engineering Scaffold," *RSC Advances* 6 (2016): 110557–110565, <https://doi.org/10.1039/C6RA17718B>.
202. H. Kobayashi, D. Terada, Y. Yokoyama, et al., "Vascular-Inducing Poly (Glycolic Acid)-Collagen Nanocomposite-Fiber Scaffold," *Journal of Biomedical Nanotechnology* 9 (2013): 1318–1326, <https://doi.org/10.1166/jbn.2013.1638>.
203. Y. Yoon, C. H. Kim, J. E. Lee, et al., "3D Bioprinted Complex Constructs Reinforced by Hybrid Multilayers of Electrospun Nanofiber Sheets," *Biofabrication* 11 (2019): 025015, <https://doi.org/10.1088/1758-5090/ab08c2>.
204. J. V. John, A. McCarthy, H. Wang, et al., "Freeze-Casting With 3D-Printed Templates Creates Anisotropic Microchannels and Patterned Macrochannels Within Biomimetic Nanofiber Aerogels for Rapid Cellular Infiltration," *Advanced Healthcare Materials* 10 (2021): 2100238, <https://doi.org/10.1002/adhm.202100238>.
205. J. A. Smith and E. Mele, "Electrospinning and Additive Manufacturing: Adding Three-Dimensionality to Electrospun Scaffolds for Tissue Engineering," *Frontiers in Bioengineering and Biotechnology* 9 (2021): 674738, <https://doi.org/10.3389/fbioe.2021.674738>.
206. Y. Xu, Q. Saïding, X. Zhou, J. Wang, W. Cui, and X. Chen, "Electrospun Fiber-Based Immune Engineering in Regenerative Medicine," *Smart Medicine* 3 (2024): e20230034, <https://doi.org/10.1002/SMMD.20230034>.
207. L. Sun, H. Chen, D. Xu, R. Liu, and Y. Zhao, "Developing Organ-on-Chips for Biomedical Applications," *Smart Medicine* 3 (2024): e20240009, <https://doi.org/10.1002/SMMD.20240009>.